Journal of Human Evolution 162 (2022) 103112

Contents lists available at ScienceDirect

Journal of Human Evolution

journal homepage: www.elsevier.com/locate/jhevol

Covariation between the cranium and the cervical vertebrae in hominids

Mikel Arlegi [a, b, *], Ana Pantoja-Pérez [c], Christine Veschambre-Couture [d], Asier Gómez-Olivencia [e, f, c]

[a] Institut Català de Paleoecologia Humana i Evolució Social (IPHES-CERCA), Zona Educacional 4, Campus Sescelades URV (Edifici W3), 43007 Tarragona, Spain
[b] Universitat Rovira i Virgili, Department d'Història i Història de l'Art, Avinguda de Catalunya 35, 43002 Tarragona, Spain
[c] Centro UCM-ISCIII de Investigación sobre Evolución y Comportamiento Humanos, Avda. Monforte de Lemos 5 (Pabellón 14), 28029 Madrid, Spain
[d] UMR 5199 PACEA, Université de Bordeaux, Allée Geoffroy Saint Hilaire, Bâtiment B8, CS 50023, 33615, Pessac Cedex, France
[e] Departamento de Geología, Facultad de Ciencia y Tecnología, Universidad del País Vasco-Euskal Herriko Unibertsitatea (UPV/EHU), Barrio Sarriena S/n, 48940 Leioa, Spain
[f] Sociedad de Ciencias Aranzadi, Zorroagagaina 11, 20014 Donostia-San Sebastián, Spain

ARTICLE INFO

Article history:
Received 30 June 2020
Accepted 26 October 2021
Available online 8 December 2021

Keywords:
Covariation
Phylogeny
Neck
Apes

ABSTRACT

The analysis of patterns of integration is crucial for the reconstruction and understanding of how morphological changes occur in a taxonomic group throughout evolution. These patterns are relatively constant; however, both patterns and the magnitudes of integration may vary across species. These differences may indicate morphological diversification, in some cases related to functional adaptations to the biomechanics of organisms. In this study, we analyze patterns of integration between two functional and developmental structures, the cranium and the cervical spine in hominids, and we quantify the amount of divergence of each anatomical element through phylogeny. We applied these methods to three-dimensional data from 168 adult hominid individuals, summing a total of more than 1000 cervical vertebrae. We found the atlas (C1) and axis (C2) display the lowest covariation with the cranium in hominids (*Homo sapiens*, *Pan troglodytes*, *Pan paniscus*, *Gorilla gorilla*, *Gorilla beringei*, *Pongo pygmaeus*). *H. sapiens* show a relatively different pattern of craniocervical correlation compared with chimpanzees and gorillas, especially in variables implicated in maintaining the balance of the head. Finally, the atlas and axis show lower magnitude of shape change during evolution than the rest of the cervical vertebrae, especially those located in the middle of the subaxial cervical spine. Overall, results suggest that differences in the pattern of craniocervical correlation between humans and gorillas and chimpanzees could reflect the postural differences between these groups. Also, the stronger craniocervical integration and larger magnitude of shape change during evolution shown by the middle cervical vertebrae suggests that they have been selected to play an active role in maintaining head balance.

1. Introduction

The relationship between form and function is present in many biological structures (e.g., Preuschoft, 2004; Ercoli et al., 2012; Hutchinson, 2012). In human evolution, one of the most explored topics is the study of morphological changes that may have occurred as an adaptation to bipedal locomotion (Robinson, 1972; Bramble and Lieberman, 2004; Sockol et al., 2007; Lovejoy et al., 2009a, b, c; Warrener et al., 2015; Ryan and Sukhdeo, 2016; Ryan et al., 2018). Those studies largely focused on anatomical elements directly related to locomotion, such as the pelvis and lower limbs (Stern, 2000; Pontzer et al., 2009; Grabowski et al., 2011; Grabowski and Roseman, 2015). However, in recent years, the number of studies regarding the vertebral column has increased, with most studies focusing on the lumbar region and giving special attention to differences in the degree of lordosis both between sexes and across hominin species (Whitcome et al., 2007; Been et al., 2012, 2014; Gómez-Olivencia et al., 2017) and some on the thoracic region (e.g., Bastir et al., 2014, 2017; Been et al., 2017; Gómez-Olivencia et al., 2018).

* Corresponding author.
E-mail address: mikelarlegui@hotmail.com (M. Arlegi).

https://doi.org/10.1016/j.jhevol.2021.103112

The literature regarding the cervical region in primates was, until recently, relatively scarce compared with the other spinal regions (e.g., Schultz, 1942, 1961; Slijper, 1946; Francis, 1955a, b; Toerien, 1957, 1961; Jenkins, 1969). More recently, the interest in this region has increased, in particular with studies analyzing the morphofunctional interactions with posture and locomotion (Manfreda et al., 2006; Mitteroecker et al., 2007; Been et al., 2014; Nalley and Grider-Potter, 2017; Arlegi et al., 2017, 2018; Meyer et al., 2018) and the relationship with the cranium (Nalley and Grider-Potter, 2015, 2019; Villamil, 2018). These (and other) studies have used several perspectives to evaluate this functional relationship not only in primates but also in other mammal groups: for example, approaches based on the biomechanical analysis of the cranium (Demes, 1985); kinematic analyses of this complex in the wild and in captivity (Bramble, 1989; Strait and Ross, 1999; Dunbar and Badam, 2000; Cromwell et al., 2001; Choi et al., 2003; Dunbar et al., 2008; Zubair et al., 2019); analyses from radiographs, photographs, electronic sensors, and dissections (Vidal et al., 1986; Graf et al., 1995a, b; Benoit et al., 2020; Jorissen et al., 2020); approaches based on the morphological correlation and integration among traits (Nalley and Grider-Potter 2015; Villamil, 2018); and musculoskeletal analyses to define modules in the craniocervical complex (Diogo et al., 2008, 2017; Diogo and Wood, 2011; Esteve-Altava et al., 2015; Arnold et al., 2017a; Powell et al., 2018; Boyle et al., 2020).

Broadly, these studies revealed that despite postural differences in mammals, no substantial differences exist among taxa in maintaining cranial balance against gravity at rest (Vidal et al., 1986; Graf et al., 1995a, b). In this passive posture, the mammal neck adopts an s-shaped vertical position to minimize the distance between the mass of the head and the weight-bearing cervicothoracic junction, thus reducing dorsal neck muscular stress (Vidal et al., 1986; Graf and Wilson, 1989). In quadrupeds, the vertical position of the neck requires high dorsiflexion of the cervicothoracic articulation (C6–T2) and hyperextension of the atlanto-occipital joint, which also allows the adjustment of head orientation and gaze (Vidal et al., 1986; White and Panjabi, 1990; Graf et al., 1995a; Nalley and Grider-Potter, 2019). The important functional role played by the cranial and caudal cervical modules contrasts with the mid-cervical module, which is mainly circumscribed to axial rotation and does not show functional specializations (Graf et al., 1995a, b; Arnold, 2020). However, species that do not display a complete quadrupedal posture, such as some primates, and especially modern humans, show a more limited range of motion in the atlanto-occipital articulation; thus, they circumscribe most of the craniocervical motions in the midsagittal plane to the cervicothoracic articulation (White and Panjabi, 1990; Graf et al., 1995a, b). The relatively slight differences observed at rest between quadrupedal and nonquadrupedal mammals increase during locomotion. The former reorients the neck horizontally during exertion, whereas humans and plausibly other upright mammals do not (Vidal et al., 1986; Graf et al., 1995a, b; Dunbar and Badam, 1998; Strait and Ross, 1999).

The concepts of integration and modularity refer to the degree of interaction between the characters of one or more anatomical structures (Olson and Miller, 1958). Both concepts have been defined as important in the phenotypic evolution of organisms from a developmental, genetic, and/or functional point of view (e.g., Olson and Miller, 1958; Cheverud, 1996; Wagner, 1996; Goswami et al., 2014). Morphological integration describes high degree of correlation within subsets of morphological traits, which may result in long-term coevolution (Cheverud, 1996). Modularity refers to the relative independence of traits that are part of different developmental or functional regions. In evolutionary studies, these concepts are crucial for the reconstruction and understanding of how morphological changes occur in organisms because they can facilitate or restrict the evolution of their characters in specific directions (Wagner, 1996; Hallgrímsson et al., 2007; Goswami and Polly, 2010; Gómez-Robles and Polly, 2012).

Because integration can enhance or constraint morphological evolution, establishing how patterns of integration have evolved concurrently with the morphology can help determine the evolution of a group (Wagner, 1988; Grabowski et al., 2011). In general terms, it has been proposed that integration patterns are relatively constant in species (Goswami, 2006; Porto et al., 2009; Bardua et al., 2019; Watanabe et al., 2019). However, both the patterns and the magnitudes of integration may vary across species (Marroig and Cheverud, 2001; Marroig et al., 2009; Porto et al., 2009; Goswami and Polly, 2010). Detecting potential differences in integration patterns is critical because these changes may indicate morphological diversification as a result of possible adaptation to selection pressures affecting evolutionary trajectories, likely related to functional effects of the mechanics of organisms (Wagner and Schwenk, 2000).

The number of vertebrae in the vertebral column is regulated by the expression of the *Hox* genes, and those of the paralog groups 4 and 5 control the organization of the cervical region (Kessel and Gruss, 1991; Burke et al., 1995; Galis, 1999a; Wellik and Capecchi, 2003). In mammals, almost all species present a fixed number of seven cervical vertebrae (Bateson, 1894; Johnson and O'Higgins, 1996; Galis, 1999b; Narita and Kuratani, 2005; Varela-Lasheras et al., 2011; Buchholtz, 2014; Böhmer, 2017; Böhmer et al., 2018), which, at the same time, are internally organized into three functional and developmental modules: upper (C1–C2), middle (C3–C5), and lower cervical (C6–C7; Arnold et al., 2016; Randau et al., 2017). Other studies proposed a slightly different subdivision of the cervical spine, which includes either the cranial base (CB) as part of the upper module (i.e., CB–C1) or the cranium and thoracic spine for some species (Arnold et al., 2017a; Villamil, 2018). The cervical spine is a transitional functional region between the head and the rest of the vertebral column, where each cervical module plays a different functional role (Graf et al., 1995b; Arnold, 2020). In the synapsid/mammal transition, these functional modules did not evolve at the same time; they started with the appearance of the upper cervical module (an early atlas-dens-axis joint) and finished by the consolidation of a lower cervical module (Buchholtz et al., 2012; Arnold, 2020 and references therein).

Regarding the morphological link between the cranium and the cervical region in primates, some researchers have found certain correlations between specific characters, which could have implications for posture and locomotor behaviors (Strait and Ross, 1999; Nalley and Grider-Potter, 2017; Villamil, 2018). In general, taxa with more horizontal necks show characteristic cervical traits to avoid vertebral articular displacement (e.g., coronal orientation of the articular facts) and for the insertion of the large epaxial musculature that supports the long load arm that results from this posture (e.g., larger transverse and spinous processes; Adams and Moore, 1975; Ebraheim et al., 2008; Nalley and Grider-Potter, 2015; Arlegi et al., 2017). Villamil (2018) found that the CB and the cervical vertebrae in hominoids, especially the C1 and the central cervical vertebrae (C3–C5), are strongly integrated. However, it was concluded that body posture and locomotion are relatively weak selection pressures in the morphology of cervical vertebrae.

Studies using anatomical network analysis also searched for functional, evolutionary, and/or developmental modules in the head-neck by combining the analyses of hard (bone/cartilage) and soft tissues (muscles; Diogo et al., 2008, 2017; Diogo and Wood, 2011; Esteve-Altava et al., 2015; Powell et al., 2018; Boyle et al., 2020). These show that the head and neck muscles in primates, compared with other anatomical regions, are a better match for the

most recent molecular tree (Diogo and Wood, 2011; Boyle et al., 2020) and that this complex is mainly defined by function (Esteve-Altava et al., 2015). They further stress that modern humans have more head and neck muscles than any other primate (Powell et al., 2018), and, interestingly, this leads to the least complex and most derived musculoskeletal system in this region among hominoids (Diogo and Wood, 2011, 2017; Powell et al., 2018).

The main objective of this study is to quantify and analyze patterns of correlation and the magnitudes of integration between the morphology of the entire cranium and the cervical vertebrae in hominids. Moreover, factors that influence integration on structures in the evolutionary process, such as the effect of size and phylogeny, will be considered. Here, we test the following hypotheses:

1) The morphological differences among functional and developmental cervical modules will be reflected in the degree of craniocervical integration (e.g., Villamil, 2018).
2) Integration is expected to be stronger in species with larger musculoskeletal features in the dorsal neck, which would indicate greater mechanical bending loads in the muscles responsible for counterbalancing the gravitational forces acting on the head (Adams and Moore, 1975).
3) Despite patterns of integration being relatively constant in mammals, we expect certain differences in the pattern of craniocervical correlation among groups that show different postural and locomotor repertoires (Grabowski et al., 2011; Grabowski and Roseman, 2015).
4) The cervical vertebrae in hominids present certain evolutionary disparities (e.g., more directional or stabilizing selection), and these differences would correspond with the internal modular division of the cervical spine (Arnold, 2020 and references therein).
5) Highly integrated sets of traits are mainly aligned along the axis of size-related variation (Marroig et al., 2009; Porto et al., 2009); therefore, removing the effect of size will result in a reduction in the levels of integration (e.g., Porto et al., 2013; Arlegi et al., 2018).

2. Materials and methods

The sample studied in this work comprises the cranium and the seven cervical vertebrae of 160 adult individuals of the family Hominidae, totaling 160 crania and 1071 cervical vertebrae: 43 *Homo sapiens*, 46 *Pan troglodytes*, 12 *Pan paniscus*, 45 *Gorilla gorilla*, 8 *Gorilla beringei graueri*, 3 *Gorilla beringei*, and 3 *Pongo pygmaeus* (Supplementary Online Material [SOM] Table S1). The surface of each anatomical element was scanned in two views, cranial and caudal, using a Go!SCAN 20 (with a resolution of 0.1 mm for the vertebrae and 0.4 mm for the crania) and later virtually assembled into a single three-dimensional (3D) object using VXelements software v. 6.3 (Creaform Inc., Lévis).

Both geometric morphometric (GM) and traditional morphometric (TM) methods were used to analyze covariation between the cranium and the cervical vertebrae in Hominidae. GM methods were used to perform the analyses at the interspecific level, and TM methods were used at the intraspecific level. Before performing the analyses, landmarks that could not be captured due to damage in the bone were, if possible, estimated using bilateral symmetry and otherwise calculated using partial least squares (PLS; Bookstein et al., 1990; Rohlf and Corti, 2000). Overall, less than 2% of the total landmarks were estimated. All statistical analyses were performed in R v. 4.0.2 (R Core Team, 2020), and, more specifically, for GMs using the package 'geomorph' v. 3.2.1 (Adams et al., 2020).

2.1. Data collection

Three-dimensional landmarks representing the morphology of each anatomical element were virtually captured from the created 3D scan models: 33 landmarks in the cranium, 27 in the atlas (C1), 33 in the axis (C2), and 34 in the subaxial cervical vertebrae (C3–C7; see SOM Tables S2–S5 for landmark definitions; Figs. 1 and 2) using Viewbox 4 software v. 4.5.0 (dHAL software, Kifissia). A high percentage of C3–C5 vertebrae of *H. sapiens* present with bituberculary of the tip of the spinous process (Gómez-Olivencia et al., 2013). In these cases, the landmarks corresponding to the most dorsal point of the spinous process were placed virtually in the midsagittal line. Before performing the analyses, those landmarks that could not be captured owing to damage in the bone were estimated using bilateral symmetry if possible and otherwise were calculated using PLS regression (Bookstein et al., 1990; Rohlf and Corti, 2000). Overall, less than 2% of the total landmarks were estimated. Owing to the difficulty of obtaining individuals in the collections that included both the cranium and all seven cervical vertebrae, those that had the cranium and a minimum of five out of the seven cervical vertebrae were selected. Of the studied individuals, 88% presented the eight anatomical elements examined here (i.e., cranium and seven cervical vertebrae) and the remaining 12% ($n = 20$) only lack one or two anatomical elements.

2.2. Geometric morphometrics

All analyses using GM techniques were performed at the interspecific level including all taxa. Before performing the statistical analyses, we conducted a generalized Procrustes analysis (GPA; Rohlf and Slice, 1990) from the raw 3D coordinates of each cervical vertebra and the cranium separately including all taxa to remove the information related to size, position, and orientation.

Integration and pairwise comparisons We quantified the degree of morphological integration between shape variables that describe the different elements of the cranium and cervical vertebrae. We used the two-block PLS regression method, using the 'integration.test' function of the package 'geomorph' (Adams et al., 2020). This method uses the decomposition of the between-block covariance matrix and searches for pairs of new axes that represent the maximum amount of covariance between the two blocks. As each axis of each block (e.g., axis 1 of block 1) only correlates with the corresponding axis of the other block (e.g., axis 1 of block 2), the covariance pattern can only be analyzed by a pair of PLS axes at a time (Bookstein et al., 1990; Klingenberg and Zaklan, 2000; Rohlf and Corti, 2000). The results of this procedure are appropriate because it yields values that are unaffected by sample size or by the number of variables (Adams and Collyer, 2016). The significance was calculated by comparing the obtained PLS correlation (r_{PLS}) values with those resulting from a random permutation of the individuals in one partition relative to those in the other (Bookstein et al., 2003; Adams and Collyer, 2016). Then, to test whether each cervical vertebra presented a significantly different magnitude of integration with the cranium compared with the other vertebrae, we calculated the effect sizes of each pairwise PLS analysis using the 'compare.pls' function of 'geomorph' (Collyer et al., 2015; Adams and Collyer, 2016). This analysis, rather than using the PLS correlation coefficient, performs two-sample *Z*-tests, which are robust to differences in sample size and the number of landmarks.

Phylogenetic signal Phylogenetically related species share an evolutionary history and thus tend to display similar trait values due to their common ancestry (Felsenstein, 1985). To evaluate shape divergence over the evolution of the cranium and the

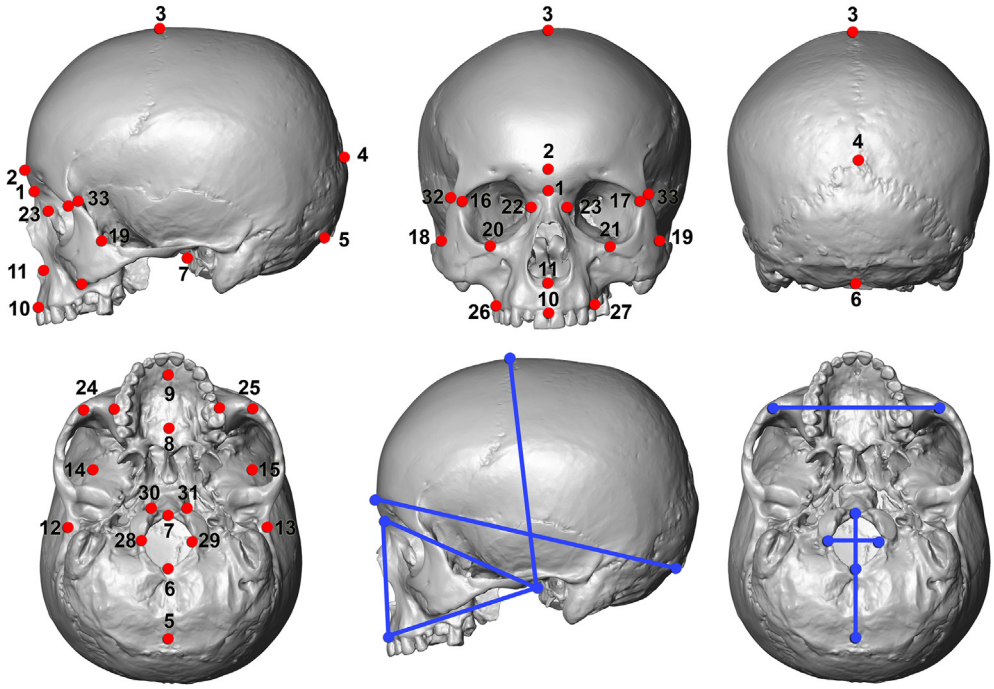

Figure 1. Landmarks (red dots) and linear measurements (blue lines) taken of the cranium in this study. Landmarks: upper left, cranium in left lateral view; lower left, in caudal view; upper center, in ventral view. Linear measurements: lower center, in left lateral view; lower center, in ventral view. Note that not all landmarks are visible in all views. See SOM Tables S2 and S6 for landmark and linear measurements definition. (For interpretation of the references to color in this figure legend, the reader is referred to the Web version of this article.)

cervical vertebrae, we calculated the phylogenetic signal of our data using the phylogenetic information of hominids from the 10kTrees Project platform (Arnold et al., 2010) and the Procrustes mean average of each species for each element independently. To estimate the phylogenetic signal, we used the function 'physignal' of 'geomorph,' which is based on the multivariate version of the K-statistic (K_{mult}: Adams, 2014). This method estimates the degree of phylogenetic signal in a data set relative to what is expected under a Brownian motion of evolution. Conversely to previous methods, K_{mult} is appropriate for highly dimensional multivariate data avoiding type I errors. Significance was estimated via shape data permutation among the tips of the phylogeny (Adams, 2014; Adams and Collyer, 2019). Finally, we explored patterns of cranial and cervical vertebrae shape evolution by projecting the phylogeny onto the morphological morphospace represented by the first two principal components (PC1 and PC2).

Phylogenetic PLS analysis To account for relatedness among the hominid species in our sample, we calculated craniocervical integration while accounting for the phylogenetic relationships among taxa using phylogenetic PLS analyses. This approach, implemented in the function 'phylo.integration' of 'geomorph,' also displays appropriate type I error rates and constant levels of integration irrespective of the number of species or trait dimensions (Adams and Felice, 2014). The significance of the analyses was performed via permutation analysis in the same way as for the PLS analysis (discussed earlier).

2.3. Traditional morphometry

All analyses from the Traditional morphometry section were performed at the intraspecific level, that is, including only the three species with the greatest sample sizes (i.e., *H. sapiens*, *G. gorilla*, and *P. troglodytes*). Here, we analyzed covariation between the cranium and the cervical vertebrae using linear measurements from both raw data sets and size-adjusted (removing the influence of size). First, linear measurements were derived from the 3D coordinates using the 'interlmkdist' function of 'geomorph.' These linear variables were selected from a series of standard measurements that best represent the morphology of the cranium and each cervical vertebra (SOM Tables S6 and S7; McCown and Keith, 1939; Martin and Saller, 1957; Howells, 1973; Bräuer, 1988). Six variables were selected for the atlas (C1), nine for the axis (C2), and another nine for each of the C3–C7 vertebrae (Fig. 3). Correlation analyses between two elements require that they both have the same number of variables, so the nine variables selected for the cranium were reduced to six for the analyses with the atlas (SOM Table S8). After that, to test whether sex was a significant source of variation in the data sets that needed to be removed, we accounted for the relative amount of shape variation attributable to sex on each vertebral and cranial element per species by creating a linear model and estimating the probability via analysis of variance. All analyses resulted in nonsignificant differences between sexes, and thus, we did not correct sex variation from the data sets.

PLS integration analysis With the obtained linear variables from the raw 3D coordinates, we first analyzed the magnitudes of integration between the cranium and the cervical vertebrae in the three species using the 'integration.test' function of 'geomorph,' the same method applied for GMs (discussed earlier).

Between variables pairwise correlation test Next, we analyzed patterns of correlation between the cranium and the cervical vertebrae in the three species by quantifying the correlation between pairs of variables. To do so, we calculated the Pearson correlation coefficient and significance between all the cranial variables, on the one side, and all the variables of each vertebra, on the other side, using the 'cor.test' function of the R package 'stats' v. 4.0.2 (R Core Team, 2020).

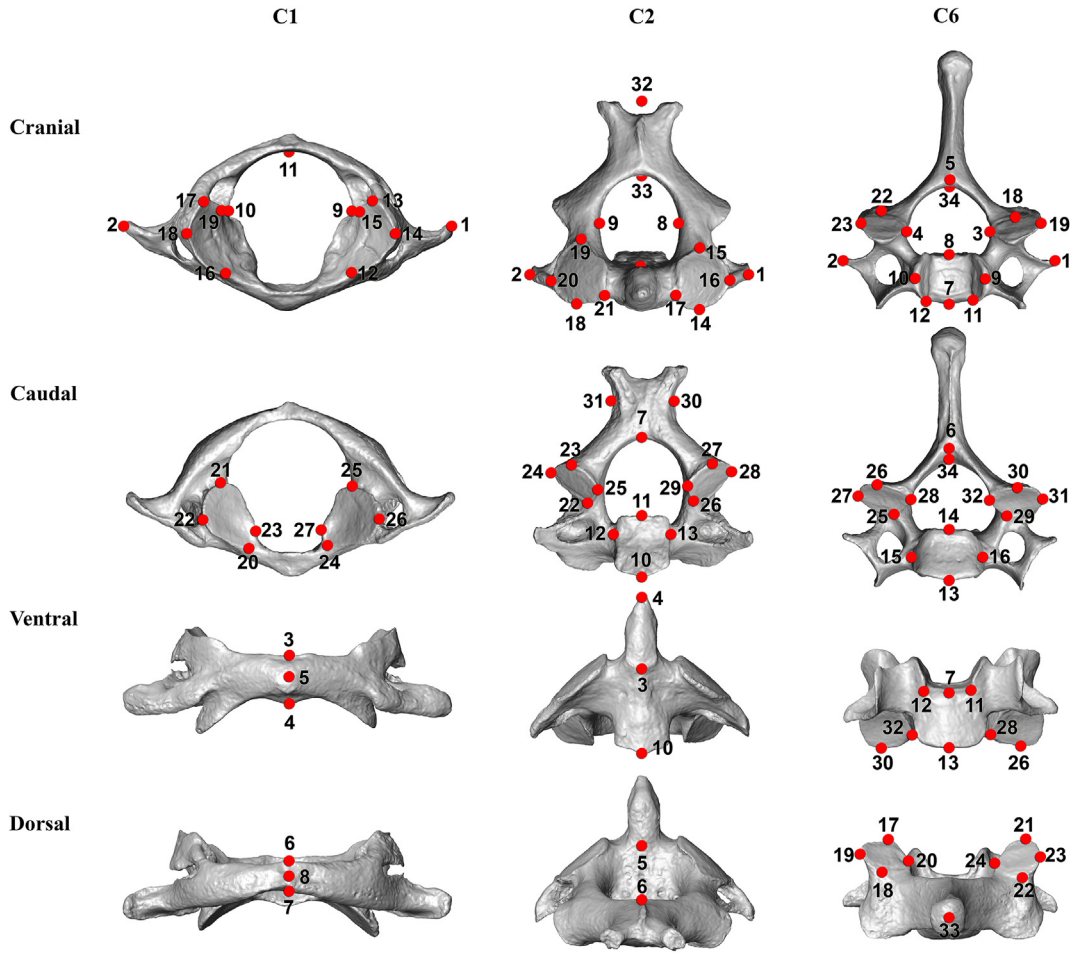

Figure 2. Landmarks used in this study in the cervical vertebrae. Note that not all landmarks are visible in all views. See SOM Table S3 for landmark definition. The figured vertebrae belong to *Pan troglodytes*.

Influence of size Next, we assessed the potential influence of size on integration. To do so, we calculated the geometric mean of each anatomical element (cranium and cervical vertebrae) using their linear measurement values (six for the atlas and nine for each of the other elements), and we used it as a proxy for size (Darroch and Mosimann, 1985; Jungers et al., 1995). To obtain 'size-corrected' data sets, we divided the raw values of the linear measurements by the geometric mean for each vertebra and the cranium (Coleman, 2008; Pablos et al., 2013; Arlegi et al., 2017), hereafter size-adjusted. Then, we repeated the two previous analyses (i.e., 'integration.test' and 'cor.test') using the obtained size-adjusted data sets. In addition, we analyzed the amount of cervical shape variation explained by cranial size (i.e., allometry) and the differences in the allometric pattern among species. To do so, we performed a regression analysis using the linear measurements from the raw data sets as dependent variables and the cranial size represented by the geometric mean as the independent variable using the 'procD.lm' function of 'geomorph' and the 'pairwise' function of 'RRPP' v. 0.6.2 (Collyer and Adams, 2018, 2021) to calculate the angle between the male and female regression vectors and its significance.

2.4. Repeatability of the data sets

Finally, to ascertain the reliability of our results, and following Melo et al. (2016), we tested the repeatability of the raw data sets (e.g., C3 *G. gorilla*, C4 *P. troglodytes*) by bootstrapping each data set 10,000 times and comparing the original and the obtained covariances matrix using random skewers analysis (mean = 0.880, median = 0.881; SOM Table S9).

3. Results

3.1. Geometric morphometrics

Interspecific integration and pairwise comparisons All analyses yielded high and significant results (Table 1), with craniocervical magnitudes of integration ranging between r_{PLS} = 0.503 (cranium/atlas) and r_{PLS} = 0.832 (cranium/C6). The atlas and axis revealed the lowest values of craniocervical covariation followed by the C7 and C3. Thus, central cervical vertebrae (i.e., C4–C6) showed higher values of covariation with the cranium than those located more peripherally in the cervical spine. The altas and axis yielded significantly different values of magnitudes of craniocervical integration compared with the rest of the vertebrae (Table 2). The rest of the pairwise comparison did not reveal significant differences among them; however, it is worth remarking that the lowest differences were obtained among middle cervical vertebrae (i.e., C4–C6). These results relatively support our hypothesis that the degree of craniocervical integration would be different between vertebrae from different cervical modules.

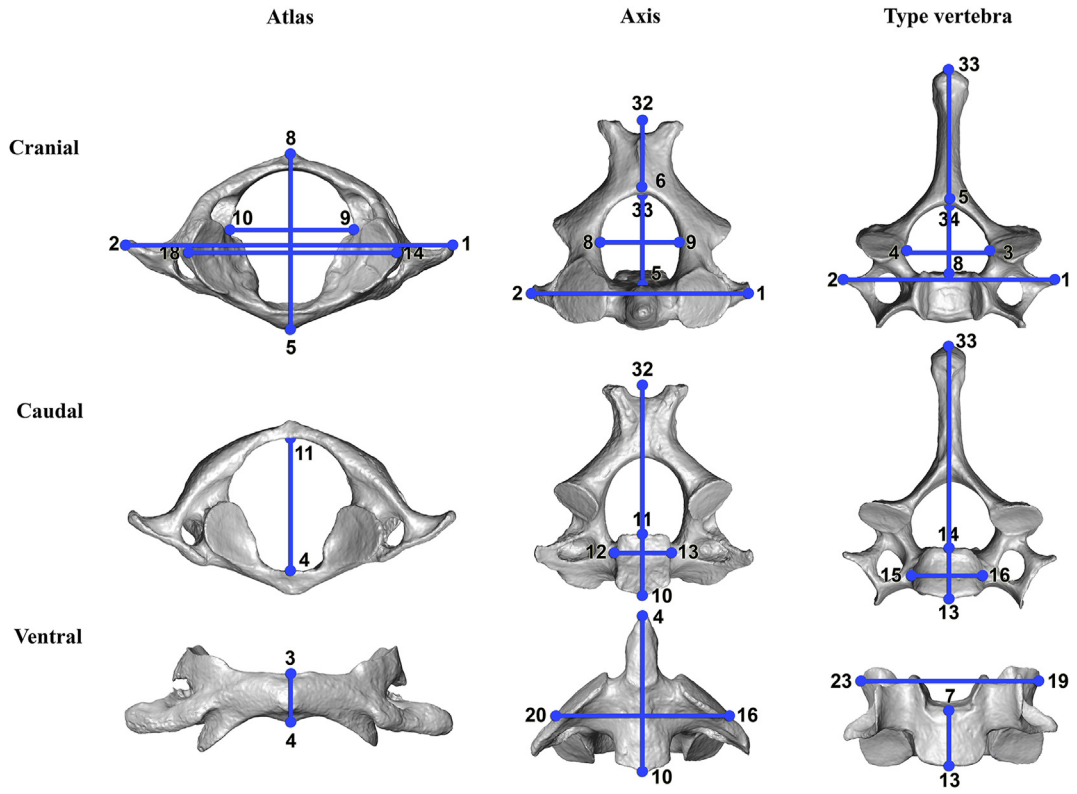

Figure 3. Linear measurements of the cervical vertebrae used in this study. The numbers indicate the landmarks from which the linear measurements have been calculated.

Table 1
Integration values (r_{PLS}), effect sizes, and standard errors (SE) between the cranium (Cr) and the cervical vertebrae (C1−C7) at the interspecific level (Hominidae).[a]

	r_{PLS}	*p*	Effect size	SE
Cr/C1	**0.503**	**<0.001**	4.026	0.004
Cr/C2	**0.594**	**<0.001**	5.874	0.003
Cr/C3	**0.772**	**<0.001**	7.200	0.003
Cr/C4	**0.825**	**<0.001**	7.587	0.004
Cr/C5	**0.776**	**<0.001**	6.014	0.004
Cr/C6	**0.832**	**<0.001**	7.506	0.004
Cr/C7	**0.707**	**<0.001**	5.544	0.004

[a] Significant values are indicated in bold (*p*-value < 0.05).

Table 2
Pairwise differences in PLS effect sizes comparing levels of craniocervical morphological integration in hominids.[a]

	Cr/C1	Cr/C2	Cr/C3	Cr/C4	Cr/C5	Cr/C6	Cr/C7
Cr/C1		0.062	**<0.001**	**<0.001**	**<0.001**	**<0.001**	**<0.001**
Cr/C2	1.867		**0.003**	**<0.001**	**0.001**	**<0.001**	0.059
Cr/C3	**4.697**	**2.926**		0.314	0.625	0.359	0.357
Cr/C4	**5.522**	**3.832**	1.006		0.602	0.928	0.063
Cr/C5	**5.113**	**3.376**	0.488	0.521		0.666	0.168
Cr/C6	**5.455**	**3.756**	0.917	0.090	0.432		0.075
Cr/C7	**3.632**	1.891	0.921	1.861	1.380	1.779	

[a] Significant values are indicated in bold (*p*-value <0.05). Values are represented in the lower diagonal, and *p*-values in the upper diagonal.

Phylogenetic signal The results of the phylogenetic analyses are shown in Table 3. They revealed that only the cranium, C3, and C4 vertebrae shapes exhibited significant (though weak) phylogenetic signal, indicating that cranial and cervical vertebrae shapes from these taxa resemble each other less than expected under the Brownian motion model of evolution. The atlas and axis exhibited the lowest values (K_{mult} = 0.052 and 0.058, respectively) and the cranium the highest (K_{mult} = 0.337), indicating lower and higher magnitudes of shape change during evolution, respectively. The subaxial cervical vertebrae displayed a trend that increases from C3 to C4 (maximum value, K_{mult} = 0.296) and then decreases toward C7 (minimum value, K_{mult} = 0.112). This supports our hypothesis that cervical vertebrae in hominids present a divergence in the magnitudes of evolutionary variation.

Table 3
Phylogenetic signal of the cranium and cervical vertebrae in hominids represented in K_{mult} values.

	Phylogenetic signal	*p*	Effect size
Cranium	**0.337**	**0.033**	1.667
C1	0.052	0.479	0.043
C2	0.058	0.239	0.557
C3	**0.186**	**0.028**	1.757
C4	**0.296**	**0.020**	1.691
C5	0.283	0.064	1.796
C6	0.226	0.063	1.762
C7	0.112	0.085	1.323

Significant values are indicated in bold (*p*-value <0.05).

Phylomorphospaces Visual information of the phylomorphospaces is shown in Figure 4. If the magnitudes of phylogenetic signal (discussed earlier) indicates the magnitude and the direction of shape divergence in the process of evolution (Klingenberg and Gidaszewski, 2010), the phylomorphospaces allow one to visualize the history of morphological diversification of a clade (Sidlauskas, 2008). In Figure 4, we can observe that the cranium and the subaxial cervical vertebrae show a similar evolutionary

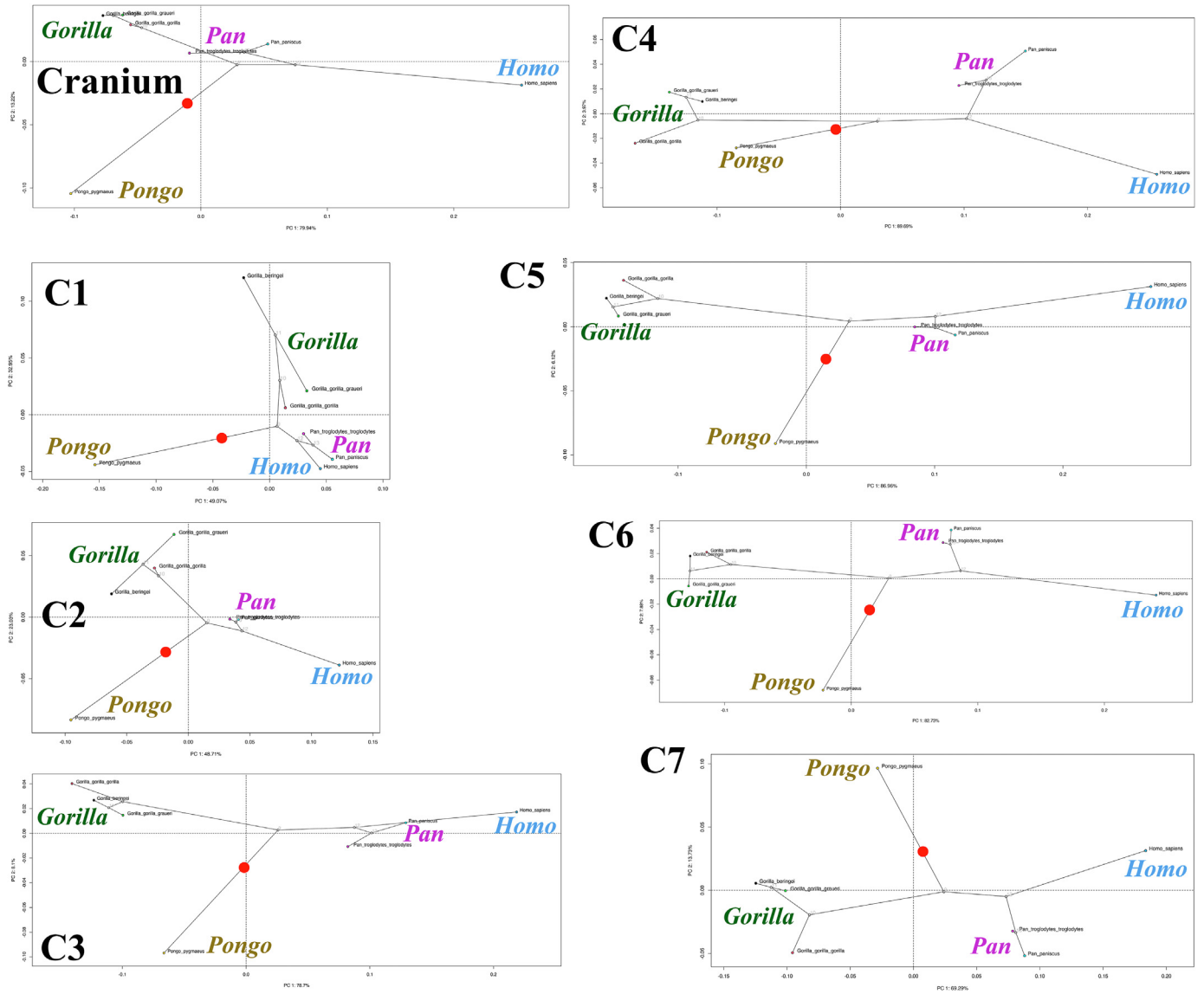

Figure 4. Phylomorphospaces of the cranium and the seven cervical vertebrae in Hominidae. The phylogenetic tree of this family was superimposed onto the first two principal components of each anatomical element. The red dot indicates the root of the tree, and the numbers on the branches (internal nodes) represent the last common ancestors for the respective pairs of lineages. (For interpretation of the references to color in this figure legend, the reader is referred to the Web version of this article.)

trend. Hominine groups are separated along, and almost in parallel, the axis of the PC1, showing a strong divergence in opposite directions for gorillas and humans. The genus *Pongo* diverges from the rest of the family, mostly in the direction of the PC2. In the atlas, *P. paniscus* and *H. sapiens* on the one hand, and *P. troglodytes* and gorillas on the other hand, show shorter distances between them than with respect to their common ancestor, indicating a certain homoplasy in shape. Finally, it is difficult to ascertain the evolutionary ratio based only on the phylomorphospaces; however, except for the atlas, the longer branches of humans indicate faster divergence in this species than those of the other taxa.

Phylogenetic PLS The results of the phylogenetic PLS analyses are shown in SOM Table S10. All pairwise tests yielded high and significant values ($r_{PLS} > 0.965$). In contrast to the phylogenetic uncorrected analyses, none of the vertebrae showed significant differences in the r_{PLS} values compared with the rest of the vertebrae.

3.2. Traditional morphometric analyses of raw data

This section presents the integration analyses between the cranium and the cervical vertebrae based on linear variables at the intraspecific level. For this purpose, only the three species with larger sample sizes (*H. sapiens*, *P. troglodytes*, and *G. gorilla*) were assessed.

PLS integration analysis The results of the PLS analysis from raw data are presented in Table 4 and Figure 5. They show that all cervical vertebrae, except for the atlas in humans and chimpanzees, were significantly integrated with the cranium for the three species. The three groups showed lower values in the atlas, which significantly differ from the rest of the vertebrae, except for the C3 in gorillas (SOM Table S11). In general terms, gorillas possessed the highest values of covariation, followed by chimpanzees and humans. Overall, the pattern of changes in the magnitudes of covariation moving down the vertebral column was similar in different species, but with a different magnitude of

Table 4
Integration values (r_{PLS}), effect sizes (E-size), and standard errors (SE) from the covariation analysis between the cranium and the cervical vertebrae at the intraspecific level based on linear measurements from raw and size-adjusted (without the influence of size) data sets.

	Homo sapiens				*Pan troglodytes*				*Gorilla gorilla*			
	r_{PLS}	p	E-size	SE	r_{PLS}	p	E-size	SE	r_{PLS}	p	E-size	SE
Raw												
Cr/C1	0.206	0.856	−0.999	0.012	0.257	0.488	−0.143	0.010	**0.552**	**0.001**	4.324	0.012
Cr/C2	**0.589**	**0.009**	2.733	0.012	**0.774**	**0.001**	5.671	0.010	**0.861**	**0.001**	8.562	0.011
Cr/C3	**0.537**	**0.021**	2.278	0.011	**0.575**	**0.001**	3.609	0.010	**0.716**	**0.001**	6.182	0.011
Cr/C4	**0.549**	**0.010**	2.739	0.011	**0.722**	**0.001**	5.709	0.010	**0.862**	**0.001**	8.274	0.011
Cr/C5	**0.533**	**0.018**	2.319	0.011	**0.707**	**0.001**	5.388	0.010	**0.880**	**0.001**	8.792	0.011
Cr/C6	**0.534**	**0.026**	2.042	0.012	**0.708**	**0.001**	4.975	0.010	**0.881**	**0.001**	8.503	0.011
Cr/C7	**0.566**	**0.008**	2.745	0.011	**0.712**	**0.001**	5.246	0.010	**0.866**	**0.001**	8.036	0.011
						Size-adjusted						
Cr/C1	0.364	0.612	−0.318	0.014	0.433	0.190	0.894	0.012	**0.620**	**0.004**	3.363	0.013
Cr/C2	0.548	0.217	0.768	0.014	0.589	0.068	1.489	0.012	**0.664**	**0.001**	3.997	0.012
Cr/C3	0.413	0.678	−0.514	0.013	**0.511**	**0.045**	1.885	0.010	**0.571**	**0.006**	2.787	0.012
Cr/C4	0.450	0.632	−0.358	0.013	**0.602**	**0.004**	2.905	0.011	**0.702**	**0.001**	4.559	0.011
Cr/C5	0.446	0.446	0.102	0.013	0.516	0.090	1.376	0.011	**0.704**	**0.001**	4.636	0.011
Cr/C6	0.464	0.306	0.479	0.013	0.407	0.663	−0.450	0.011	**0.707**	**0.001**	4.613	0.011
Cr/C7	0.434	0.499	−0.075	0.013	0.421	0.526	−0.106	0.011	**0.687**	**0.001**	4.347	0.011

Significant values are indicated in bold (p-value <0.05).

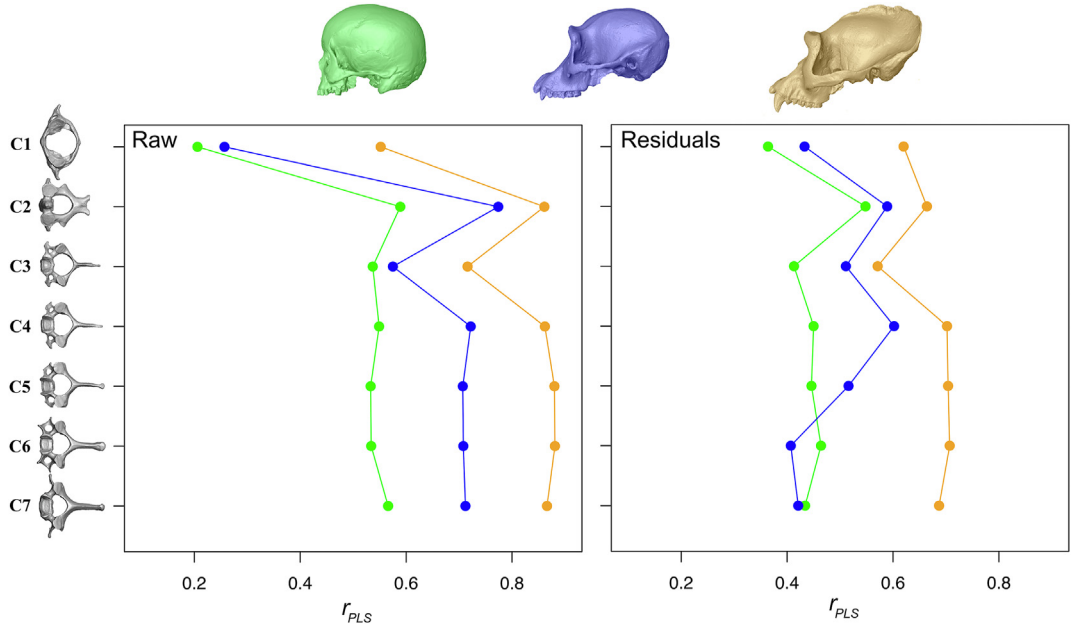

Figure 5. Correlation analysis between the cervical vertebrae and the skull from raw data (left) and size-adjusted (right) in *Homo sapiens* (green), *Pan troglodytes* (blue), and *Gorilla gorilla* (light yellow). The numerical values are represented in Table 4. The cervical vertebrae represented in the figure belong to an individual of the species *P. troglodytes*. Abbreviation: r_{PLS} = Partial least square correlation. (For interpretation of the references to color in this figure legend, the reader is referred to the Web version of this article.)

integration, except for the C3 in humans, which departed the pattern followed by chimpanzees and gorillas (Fig. 5). Pairwise comparisons among the three species revealed that gorillas significantly differ from humans and chimpanzees in the craniocervical magnitude of integration in the seven cervical vertebrae (SOM Table S12). In contrast, humans and chimpanzees only displayed significant differences in those vertebrae located in the midlower cervical spine (i.e., C4, C5, and C6). These results support the hypothesis that species with larger musculoskeletal features in the dorsal neck display a higher degree of integration.

Between variables pairwise correlation test The results revealed that the correlation between the cranium and the cervical vertebrae in the three species occurred at different degrees and among different traits (Table 5 and Fig. 6; SOM Table S13). In general terms, in gorillas and chimpanzees, the highest craniocervical correlations were shown between either the length of the CB or the length of the face in the cranium and the maximum dorsoventral or transversal diameter traits in the cervical vertebrae (Table 5). In humans, in contrast, a clear correlation pattern did not exist between craniocervical variables. Indeed, in this taxon, the stronger correlation values were displayed in traits related to maximum cranial length and vertebral body height, transverse, and dorsoventral diameter (i.e., M1, M5, and M8). Also, we can observe how, besides magnitude of integration (higher values in gorillas), gorillas and chimpanzees present a more similar pattern of correlation among craniocervical traits throughout the cervical spine compared with humans. They show the highest correlations in the upper left of each diagram, where variables related to the midsagittal plane are located (Fig. 6). Conversely, in humans, the distribution of the highest correlations is not concentrated in that area of the diagram and shows a more heterogeneous pattern throughout the cervical region. These

Table 5
Highest correlation values between the cranium and cervical variables in *Homo sapiens*, *Pan troglodytes*, and *Gorilla gorilla* from raw data sets.

H. sapiens	Highest correlation	r	*p*	2nd Highest correlation	r	*p*
Cr/C1	Basion-Prosthion/MaxDvDi	0.251	0.113	Zygo-Zygo/STrD	0.237	0.148
Cr/C2	Zygo-Zygo/STrD	**0.528**	**<0.001**	Glabella-Inion/M1a	**0.518**	**0.001**
Cr/C3	Glabella-Inion/M5	**0.513**	**<0.001**	Opisthion-Basion/M11	**0.470**	**0.001**
Cr/C4	Glabella-Inion/M8	**0.547**	**<0.001**	Nasion-Prosthion/STrD	**0.536**	**<0.001**
Cr/C5	Glabella-Inion/M5	**0.549**	**<0.001**	Opisthion-Basion/M11	**0.525**	**<0.001**
Cr/C6	Nasion-Prosthion/M1	**0.546**	**<0.001**	Glabella-Inion/MaxTrDi	**0.466**	**0.002**
Cr/C7	Glabella-Inion/STrD	**0.538**	**<0.001**	Nasion-Prosthion/MaxTrDi	**0.516**	**<0.001**
P. troglodytes	Highest correlation	r	*p*	2nd Highest correlation	r	*p*
Cr/C1	Opisthion-Basion/M11	0.306	0.051	Opisthion-Basion/MaxTrDi	0.281	0.076
Cr/C2	Basion-Prosthion/MaxTrDi	**0.653**	**<0.001**	Basion-Prosthion/MaxDvDi	**0.648**	**<0.001**
Cr/C3	Basion-Prosthion/MaxTrDi	**0.647**	**<0.001**	Opisthion-Basion/M10	**0.516**	**<0.001**
Cr/C4	Basion-Prosthion/MaxDvDi	**0.672**	**<0.001**	Nasion-Basion/M5	**0.579**	**<0.001**
Cr/C5	Basion-Prosthion/MaxDvDi	**0.631**	**<0.001**	Nasion-Basion/StrD	**0.600**	**<0.001**
Cr/C6	Basion-Prosthion/MaxDvDi	**0.674**	**<0.001**	Nasion-Basion/M5	**0.603**	**<0.001**
Cr/C7	Basion-Prosthion/MaxDvDi	**0.718**	**<0.001**	Nasion-Basion/M5	**0.659**	**<0.001**
G. gorilla	Highest correlation	r	*p*	2nd Highest correlation	r	*p*
Cr/C1	Glabella-Inion/MaxTrDi	**0.621**	**<0.001**	Glabella-Inion/MaxDvDi	**0.586**	**<0.001**
Cr/C2	Nasion-Basion/MaxTrDi	**0.868**	**<0.001**	Nasion-Basion/MaxDvDi	**0.839**	**<0.001**
Cr/C3	Nasion-Basion/MaxTrDi	**0.847**	**<0.001**	Basion-Prosthion/MaxTrDi	**0.798**	**<0.001**
Cr/C4	Nasion-Basion/MaxTrDi	**0.846**	**<0.001**	Basion-Prosthion/MaxDvDi	**0.842**	**<0.001**
Cr/C5	Basion-Prosthion/MaxDvDi	**0.865**	**<0.001**	Nasion-Basion/MaxDvDi	**0.858**	**<0.001**
Cr/C6	Basion-Prosthion/M13	**0.862**	**<0.001**	Nasion-Basion/MaxDvDi	**0.851**	**<0.001**
Cr/C7	Nasion-Basion/STrD	**0.852**	**<0.001**	Basion-Prosthion/MaxDvDi	**0.851**	**<0.001**

Significant values are indicated in bold (p-value <0.05).
The vertebral dimensions follow Figure 6 and SOM Table S13.

results indicate certain differences in the craniocervical correlation pattern between species that present different postural and locomotor repertoires; however, we have not directly tested the relationship between them here. Thus, to confirm our hypothesis that certain differences in postural and locomotor repertoires would be reflected in their patterns of craniocervical integration, further analysis with a more specific approach is needed.

Allometry The results showed that all the cervical vertebrae, except the atlas in chimpanzees and humans, exhibited a significant amount of shape variation explained by cranial size (Table 6). Gorillas yielded the largest percentages of variation followed by chimpanzees. Also, the C2–C7 vertebrae presented positive allometric trends; in contrast, the atlas showed a negative trend (Fig. 7). Pairwise analyses yielded similar allometric pattern for the three species in the first (atlas) and last (C7) cervical vertebrae (Table 7). Humans differ from chimpanzees in the C4–C5 vertebrae and from gorillas in the C2–C6. Gorillas and chimpanzees differ in the allometric pattern in the C2 and C5 vertebrae.

3.3. TM analyses of size-adjusted data

Compared with the previous section on raw data, the size-adjusted data give here information on shape without the influence of size.

PLS integration analysis The results of the PLS analysis from size-adjusted databases are presented in Table 4 and Figure 5. In comparison with those results obtained from raw data sets, except for the atlas, all the cervical vertebrae obtained lower covariation values with the cranium. Gorillas displayed significant r_{PLS} values in all the covariation analyses (i.e., cranium with C1–C7) and chimpanzees in C3 and C4 vertebrae, and humans did not show significant results in any craniocervical covariation analyses (Table 4). In consequence, compared with the results obtained from the raw data set, this results in a reduction in the differences in the values of covariation among vertebrae. Also, pairwise comparisons revealed that once the size factor is removed, differences between vertebrae and species are also reduced (SOM Tables S15–16). Finally, these results partially support the hypothesis that removing the effect of size would result in a reduction of the magnitude of integration. Conversely to the rest of the vertebrae, the atlas increased its values.

Between-variables pairwise correlation test These results also confirmed this reduction of the levels of correlation from size-adjusted data sets compared with those obtained from raw data sets, except in the atlas of *H. sapiens* and *P. troglodytes* (SOM Table S16 and Fig. S1). Also, in general terms, the highest craniocervical correlation values are not related to variables representing maximum length, either midlateral (e.g., MaxTrDi, STrD, or M8) or dorsoventral (e.g., MaxDVDi, M5, or M13), but variables related to the vertebral foramen (SOM Table S17).

4. Discussion

4.1. Cranium-cervical covariation: differences between species

The cervical column of hominoids has been proposed to be highly integrated with the cranial base, with no substantial differences between species (Villamil, 2018). However, our results indicate differences exist both in the patterns of correlation and magnitudes of integration of the cervical vertebrae with the cranium as a whole (Fig. 6). Among hominines, gorillas display the highest magnitude of craniocervical integration in all the vertebrae, followed by chimpanzees. If the magnitude of integration indicates the degree of interaction between the cranium and the cervical vertebrae, the pattern reveals how this is produced (Grabowski et al., 2011). Our results showed that humans differ from both gorillas and chimpanzees in the traits that link the cranium and the cervical spine. In both gorillas and chimpanzees, the strongest correlation occurs between variables/traits representing prognathism and length of the cranial base and maximum length and width of the vertebrae. In contrast, in humans, this is produced

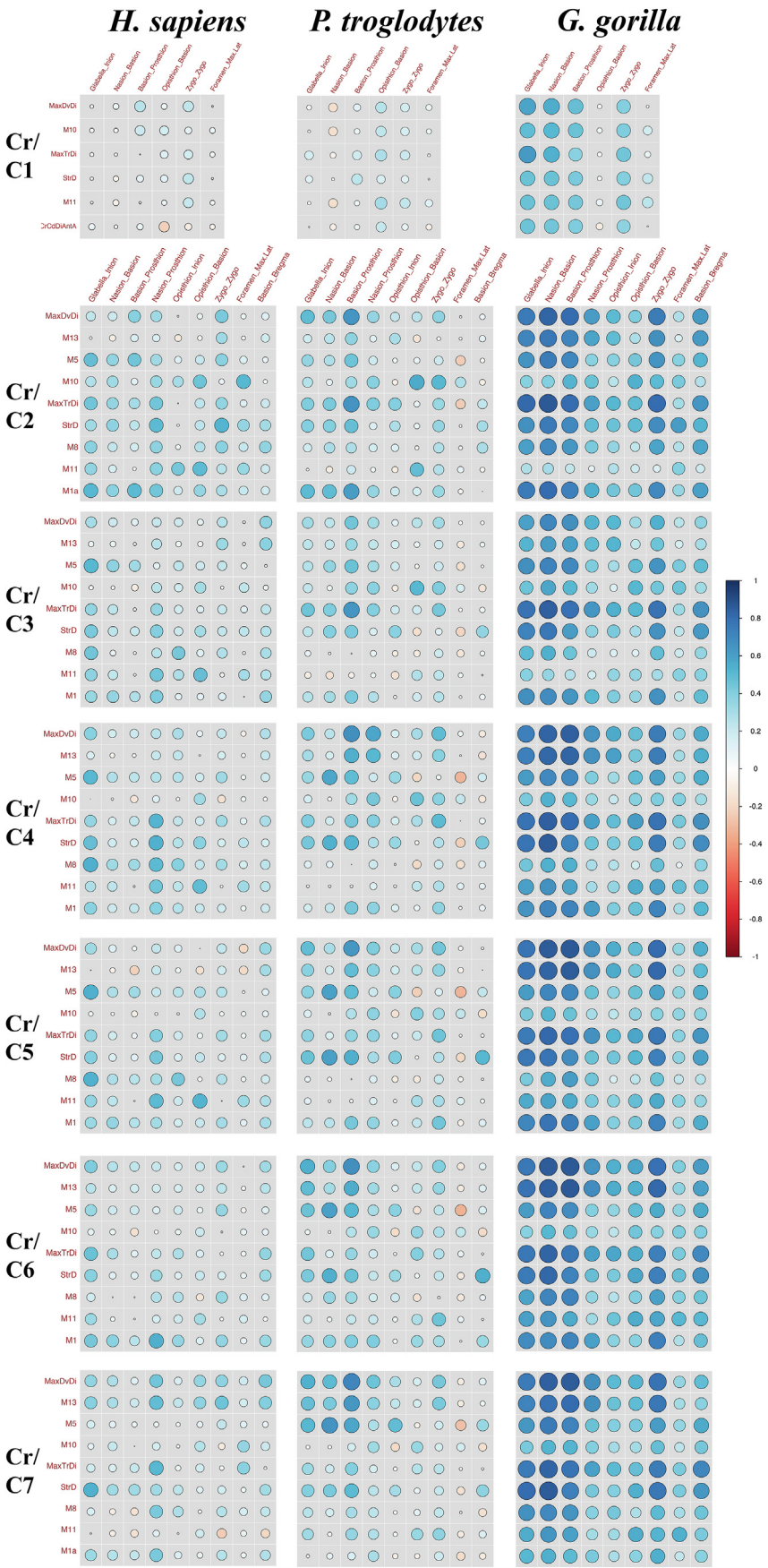
H. sapiens
P. troglodytes
G. gorilla
Cr/C1
Cr/C2
Cr/C3
Cr/C4
Cr/C5
Cr/C6
Cr/C7
Glabella_Inion
Nasion_Basion
Basion_Prosthion
Nasion_Prosthion
Opisthion_Inion
Opisthion_Basion
Zygo_Zygo
Foramen_Max.Lat
Basion_Bregma
MaxDvDi
M13
M5
M10
MaxTrDi
StrD
M8
M11
M1a
M1
1
0.8
0.6
0.4
0.2
0
-0.2
-0.4
-0.6
-0.8
-1

between the cranial length and variables related to dimensions of the vertebral body, especially in the midcervical spine. Indeed, in the case of humans, the correlation pattern is not reduced to a few variables as in gorillas and chimpanzees, but a larger range of cervical variables are associated with the cranium, resulting in a more heterogeneous correlation pattern throughout the cervical spine. These results support our hypothesis that species with large musculoskeletal complexes (i.e., gorillas and chimpanzees) would show stronger integration.

Unsurprisingly, in these quadruped species, the highest correlation occurred between variables functionally implicated in the head's load arm, such as the prognathism of the face (Schultz, 1942), and those vertebral traits that serve for the insertion of the major nuchal muscles that support this stress (i.e., transverse and spinous processes, Kapandji, 1974; White and Panjabi, 1990). On the other hand, in species with an upright posture, such as humans, where the head is located upon the cervical spine and the loads are transmitted more vertically (Demes, 1985), the highest correlation occurs between the cranial maximum length and vertebral body variables. This could reflex the different muscular (e.g., Dean, 1985a, b) and biomechanical characteristics of the head-neck movement system between these groups, as humans maintain the atlas and the lower cervical vertebrae in a midposition between extreme flexion and extreme extension (Graf et al., 1995b), resulting in a more self-stabilizing resting posture (Schultz, 1942; Adams and Moore, 1975, Dean, 1985a, b; Lieberman, 2011). This might suggest that cervical vertebral morphology is influenced by the biomechanical requirements of head movement and maintenance of the visual field, especially during locomotion, when the advantage of cervical lordosis in pronograde species is minimized owing to the reorientation of the neck (Graf et al., 1995b; Manfreda et al., 2006; Nalley and Grider-Potter, 2015; Arlegi et al., 2017); however, more specific analyses are necessary to test this observation. These results support our hypothesis that differences in postural and locomotor behaviors among groups could be reflected in their pattern of craniocervical correlation. Similarly, Nalley and Grider-Potter (2019) found a correlation between anterior cranial features that might reflect postural behaviors and cervical traits associated with the muscles involved in counterbalancing the head. Their results also revealed an influence of head shape on cervical morphology, with humans being an outlier within primates, and they suggested that neck posture during locomotion could also affect cervical morphology (Nalley and Grider-Potter, 2019).

4.2. Cranium-cervical covariation: differences between vertebrae

Our results on craniocervical integration in hominids recovered that all the cervical vertebrae are integrated with the cranium, supporting previous results obtained in hominoids between the cervical spine and the cranial base (Villamil, 2018). However, our results do not conform to Villamil's (2018) results in which cervical vertebra is the most integrated with the cranium. We obtained the lowest covariation at the interspecific and intraspecific levels in the atlas/cranium association, whereas previous results indicated the atlas was the most integrated with the cranial base (Villamil, 2018). This could be easily the result of the experimental design: we included the entire morphology of the cranium, and thus, we did not analyze the same features as Villamil (2018), who focused on the CB. Our model including the entire morphology of the cranium would mainly reflect different aspects of the biomechanics of the head balance in the craniocervical complex, whereas the focus on the cranial base would represent the biomechanical and developmental process in that specific module, which is tightly linked with the atlas.

Table 6
Results from the regression of cervical shape against cranial size for hominins.

	Homo sapiens	*p*	*Pan troglodytes*	*p*	*Gorilla gorilla*	*p*
C1	1.3	0.574	4.4	0.184	**21.1**	**0.002**
C2	**14.1**	**0.002**	**21.3**	**0.001**	**59.6**	**0.001**
C3	**10.5**	**0.005**	**13.1**	**0.005**	**45.3**	**0.001**
C4	**14.7**	**0.003**	**23.5**	**0.001**	**67.0**	**0.001**
C5	**8.9**	**0.018**	**21.1**	**0.001**	**68.0**	**0.001**
C6	**10.2**	**0.015**	**20.1**	**0.001**	**70.0**	**0.001**
C7	**15.8**	**0.002**	**20.8**	**0.001**	**63.3**	**0.001**

Significant values are indicated in bold (p-value <0.05). Values represent the percentage of shape variation in the cervical vertebrae explained by cranial size.

We also found the atlas and axis showed significantly lower magnitude of integration with the cranium than the rest of the cervical vertebrae. The stronger integration of the subaxial cervical vertebrae with the entire cranium could express higher biomechanical implications in functions related to maintaining head balance and movements and visual field. The intermediate epaxial muscles mainly implied in counter the load arm associated with head-neck posture (e.g., splenius capitis, semispinalis capitis, longissimus capitis) have their origin in the midlower cervical vertebrae and insert on the occipital bone (Kapandji, 1974; White and Panjabi, 1990). Indeed, the atlas and axis play an obvious role in stabilizing and transmitting the head mass to the rest of the vertebral column. They have their own deep muscular group formed by the suboccipital muscles (i.e., rectus and obliquus capitis), which tightly attach the first to vertebrae with the occiput (Kapandji, 1974; White and Panjabi, 1990). However, these deep muscles have short-moment arms that produce fast movements but relatively lower flexoextension moment arm compared with those from the upper muscular layers (e.g., splenius capitis, semispinalis capitis; Ackland et al., 2011). All this is reflected in the different morphology of these vertebrae, which could affect the lower degree of covariation with the entire cranium compared with the subaxial cervical vertebrae.

Despite these differences in the degree of integration between the atlas and axis, we could not detect a clear modularization of the cervical region based on the levels of covariation with the cranium. As we said, the atlas and axis clearly distinguish their magnitude of integration from the rest of the vertebrae but also present significant differences between them. Also, the subaxial cervical vertebrae exhibited lower differences between those conforming to *a priori* modules, especially those of the middle cervical region (C4–C6), leaving C3 and C7 as transitional modules. However, these divisions are not based on significant differences among them but the observed differences in the magnitude of integration with the cranium. Thus, besides a clear cranium/C1 and cranium/C2 modular distinction from the rest of the vertebrae and the slight differences between central and more caudal cervical vertebrae, we could not detect an evident modularization of the subaxial cervical spine based on their covariation with the cranium as in previous works (Arnold et al., 2016; Randau et al., 2017; Villamil, 2018). This different finding could be explained by the fact that each of these studies

Figure 6. Pairwise correlation among craniocervical variables in humans (left), chimpanzees (middle), and gorillas (left). Larger circles mean higher correlation (either positive or negative), blue color means positive correlation values, and red color negative correlation values. Small white circle means no correlation between the variables ($r = 0$). Besides differences in the magnitudes of correlation among variables (gorillas' higher values), gorillas and chimpanzees display a more similar correlation pattern than humans, showing a trend of higher correlation in variables related to the midsagittal plane (upper-left part of each scatterplot). Numerical values are shown in Table 5 and SOM Tables S22–28, and variable definitions in SOM Table S6. (For interpretation of the references to color in this figure legend, the reader is referred to the Web version of this article.)

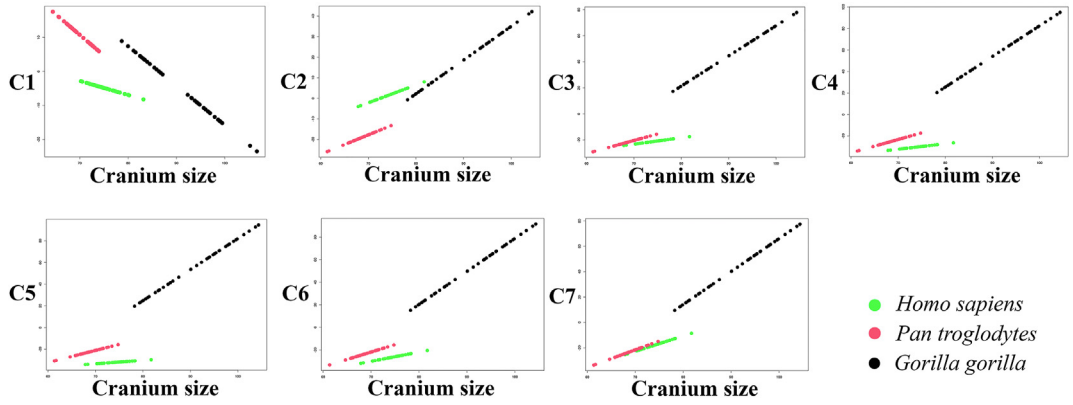

Figure 7. Allometry analyses of cervical vertebral shape (principal component 1 [PC1] for fitted values; y) against cranial size (x) using the geometric mean as proxy for size in *Gorilla gorilla*, *Pan troglodytes,* and *Homo sapiens*. For this regression visualization, we used the method 'PredLine' from the function 'procD.lm' of 'geomorph.' This method calculates fitted values from a linear model and plots the first principal component of the 'predicted' values against size showing the allometric trends in a stylized way (Adams and Nistri, 2010). All the cervical vertebrae present a positive allometric trend with the exception of the atlas. The three species show similar allometric pattern in the atlas and the C7 vertebrae (Table 7). Humans differ from gorillas in the C2–C6 and from chimpanzees in the C4–C5. Gorillas and chimpanzees show different patterns in the C2 and C5.

analyzed integration in the cervical spine from a different angle (i.e., within each vertebra, between vertebrae, with the entire cranium [or with cranial base]), which reflect different aspects of the modularity between the studied regions (developmental, functional, and/or morphological characteristics of their anatomy), and perhaps the criteria for assessing the relative independence of the modules.

4.3. The phylogenetic factor and its influence on covariation

The phylogenetic signal was weak or very weak in all the analyzed anatomical elements and only significant in the cranium, C3, and C4 vertebrae. Previous studies also found a significant phylogenetic signal in the cranium of hominoids; however, most of them focused their hypotheses on cranial developmental and functional modules such as the face and the cranial vault (von Cramon-Taubadel and Smith, 2012; Profico et al., 2017; Villamil, 2021), the cranial base (Lieberman et al., 2000), or the temporal bone (Lockwood et al., 2004). The scarce works that have quantified the phylogenetic signal in the cervical vertebrae of terrestrial mammals, including primates, found a significant phylogenetic signal in the atlas and axis (Vander Linden et al., 2019a, b), but, to our knowledge, there is no information about the subaxial cervical vertebrae. The discrepancy between these previous works and our results could be explained by the phylogenetic sample used by Vander Linden et al. (2019a, b), which included a diverse group of mammals, including primates, rodents, lagomorphs, tree shrews, and colugos. Our analysis was reduced to a single family (Hominidae) including seven taxa, and thus, these results can be considered as preliminary until further analyses including more related taxa are performed.

From our data, only two vertebrae, C3 and C4, showed a significant (although weak) phylogenetic signal, indicating the lack of congruence between the molecular and morphological data in the cervical spine under a Brownian motion model of evolution. This can be interpreted as the adaptation of cervical vertebrae to selection pressures, mainly related to functional and developmental factors. In the case of the C3 and C4, their significant phylogenetic signal could be due to their role as transitional vertebrae between the C1–C2 module and the subaxial cervical vertebrae. In general, the shape of the cervical vertebrae, especially those from the central cervical spine, rapidly diverges from their ancestry in different directions. Hominines, the clade representing humans, gorillas, and chimpanzees, mainly diverge in parallel to the first axis, suggesting a certain degree of directional selection. Integrated structures, such as the subaxial cervical vertebrae in hominines (Arlegi et al., 2018), evolve following the path of least resistance (Schluter, 1996), which is the axis representing the largest variation, a concept related to this mode of evolution. As other authors proposed, here it is also plausible that integration among traits obscures the phylogenetic signal from the data by constraining vertebral shape from evolving in a more stochastic way (Varón-González et al., 2020; Villamil, 2021). However, many other factors can also obscure the phylogenetic signal during the evolutionary process, such as reversals, homoplasies by parallel or convergent evolution, allometric effects, or nonheritable bone characters resulting from stress (Strait, 2001; Lycett and Collard, 2005; Gilbert et al., 2009; Klingenberg and Gidaszewski, 2010; Varón-González et al., 2020). Based on the low amount of shape divergence (Table 3) and the suggestion of convergent evolution in hominines (Fig. 4), the shape of the atlas might have been the subject of a stabilizing selection, which has been related to structures that show a consistent low degree of within-element integration (Steppan et al., 2002; Gómez-Robles and Polly, 2012). On the contrary, the subaxial cervical vertebrae show evidence of directional selection. Despite these differences, both modes of evolution may affect the rate and direction of evolutionary change (Hallgrímsson et al., 2002), resulting in the (almost) absence of a phylogenetic signal on the cervical vertebrae.

Apart from these evolutionary patterns of shape, the studied anatomical elements also exhibited different amounts of shape divergence in their respective morphospaces. Among the studied elements, the atlas and axis displayed the lower magnitude of shape change during evolution (Table 3 and Fig. 4). Regarding the rest of the subaxial cervical vertebrae, they revealed a trend in the amount of divergence with a steady increase from C3 to C4 and a subsequent reduction until reaching the lowest values in C7 (Fig. 4). The atlas and axis together with the cranial base have been proposed to form a functional module (de Beer, 1937; Choi et al., 2003), which could explain the relative conservatism in morphological evolution in these two vertebrae, possibly linked to maintaining the functionality of the craniocervical complex (Evans, 1939). The trend observed in the subaxial cervical spine means that the shapes of central vertebrae are probably more derived, while the morphologies of the C3 vertebra and, especially, the C7 vertebra are more conserved evolutionarily. This general pattern of evolutionary divergence in the cervical spine, from which those vertebrae located in the middle of the cervical region show directional selection and those located more peripherally a certain stabilizing selection, could indicate a certain degree of constraint in the most

Table 7
Pairwise statistics of the allometric model (see Table 6) comparing *Homo sapiens*, *Pan troglodytes*, and *Gorilla gorilla* slopes vector angles.

	C1			C2			C3			C4			C5			C6			C7		
	Angle	Z	*p*	Angle	Z	*p*	Angle	Z	*p*	Angle	Z	*p*	Angle	Z	*p*	Angle	Z	*p*	Angle	Z	*p*
Homo sapiens: *Pan troglodytes*	18.1	−0.6	0.706	19.7	0.5	0.248	34.5	1.5	0.064	**38.2**	**6.0**	**0.002**	**45.5**	**7.2**	**0.001**	18.9	1.5	0.083	18.4	0.1	0.127
Homo sapiens: *Gorilla gorilla*	14.1	−0.4	0.614	**36.2**	**4.9**	**0.001**	**41.5**	**3.2**	**0.018**	**45.7**	**9.6**	**0.001**	**54.3**	**11.3**	**0.001**	**26.5**	**4.7**	**0.005**	14.9	1.2	0.090
Gorilla gorilla: *Pan troglodytes*	9.8	−0.6	0.793	**22.4**	**1.9**	**0.036**	14.4	0.3	0.226	12.6	1.4	0.067	**17.1**	**2.7**	**0.021**	14.0	1.3	0.083	9.1	−0.1	0.447

The allometric model tests the influence of cranial size on cervical vertebrae shape.[a]
[a] Significant values are indicated in bold ($p < 0.05$).

peripheric elements within this modular structure. This characteristic was also observed in the degree of integration in other vertebral modules of the vertebral column, such as the thoracic and lumbar regions of *H. sapiens* (Arlegi et al., 2020), which was linked to the degree of functional constraint in articulated structures. Our results support the hypothesis that cervical vertebrae in hominids present certain evolutionary disparity, and these differences could correspond to the atlas and axis with the internal modular division of the cervical spine. However, despite differences among the subaxial cervical vertebrae, we could not observe a clear modular subdivision with our experimental design.

4.4. Influence of size on covariation

Similar to previous works, the results of this study also indicate that size has an important effect on increasing the strength of integration (Zelditch, 1988; Marroig et al., 2009; Porto et al., 2013; Arlegi et al., 2018, 2020). Once the effect of size was removed, all vertebrae, except for the atlas, exhibited a reduction in their magnitude of integration with the cranium in the three species. This mainly supports our hypothesis that removing the effect of size would reduce the degree of integration; however, this was not supported for the atlas. This is likely because, following our allometric results, shape variation in the atlas is not explained by cranial size in humans and chimpanzees and is lower relative to the other vertebrae in gorillas. This means that size variation in the cranium influence other cervical vertebrae (i.e., C2–C7) morphology but not the atlas, and thus removing this effect in the atlas and cranium does not negatively affect their integration. Indeed, the shape of the atlas is highly conditioned by its inherent link with the cranial base (e.g., Evans, 1939), and its functional role in the craniocervical junction may relatively constrain the influence of other sources of variation, such as cranial size.

The high variation in C2–C7 vertebral shape explained by cranial size, especially in gorillas, may be related to the primary biomechanical function of the neck, which is to balance the head (e.g., Dunbar et al., 2008). Large-bodied mammals need shorter necks to reduce the distance between the head's center of mass and the cervicothoracic junction to lower the bending moment, avoiding vertebral articular displacement (Preuschoft and Klein, 2013; Müller et al., 2021). In a similar vein, a previous study analyzing cervical craniocaudal length relative to body size revealed that in non-marsupial mammals, the atlas showed a different allometric scaling relative to the rest of the cervical vertebrae (Arnold et al., 2017b); C2–C7 vertebrae decreased in length as body size increased, whereas the atlas increased. Our allometric result indicates that beyond neck length, the overall morphology of the cervical vertebrae is also influenced by cranial size, possibly affecting each trait differently. From the three species analyzed here, gorillas clearly showed the highest craniocervical integration and the highest cervical shape variation explained by cranial size. Whether the characteristic features of the cervical morphology of gorillas, such as their large spinous processes (Schultz, 1961; Arlegi et al., 2017), are related to functional requirements to balance and stabilize the head is something that needs further analysis.

In addition, our results indicate different allometric relationship between cervical vertebrae's shape and cranial size among species in all vertebrae except in the atlas and C7 (Fig. 7 and Table 7). The largest differences occurred between gorillas and humans, the latter also yielding the lowest allometric variation in all the vertebrae. The lower influence of cranial size in cervical shape in humans may be likely related to their upright posture and bipedal locomotion. In a vertical cervical spine, the head's gravity center is closer to the atlanto-occipital joint, reducing the neck's bending moment (Schultz, 1942; Demes, 1985). This is not exclusive of

humans, as a different allometric pattern in the cervical spine compared with other mammals has also been observed in kangaroos: an upright posture and bipedal-saltatorial locomotion taxon (Arnold et al., 2017b). In addition, a positive allometric trend was observed in the atlas and axis of primates (Manfreda et al., 2006; Nalley and Grider-Potter, 2017). Manfreda et al. (2006) observed a significant link between atlas shape and body mass and also that the allometric trend was distinct between the nonhuman primates and *H. sapiens* in morphological traits related to locomotion patterns. Finally, in hominines, we also obtained a different allometric trend in the atlas of hominines compared with the rest of the cervical vertebrae. This was also observed in a previous study including a vast amount of mammal species (Arnold et al., 2017a, b), in which they observed that atlas length increased with larger body sizes. In the present study, we included the general shape of the vertebrae and not only the craniocaudal length as in the study by Arnold et al. (2017a, b), but our results indicate that the atlas shape is affected differently from body or cranial size compared with the rest of the cervical spine.

5. Conclusions

The major objective addressed in this study was to analyze the degree of covariation between the cranium and the cervical vertebrae in hominids, for which we proposed and tested five hypotheses resulting in: First, in hominids, the atlas and axis module show significantly lower values of magnitudes of craniocervical integration than the rest of the cervical vertebrae. Second, as expected, species with larger musculoskeletal features in the dorsal neck, in this case, gorillas, show the highest degree of craniocervical correlation. Third, in contraposition to gorillas and chimpanzees, modern humans showed a different pattern of craniocervical correlation, showing less specialized and more diverse association among their features. Fourth, from an evolutionary point of view, the cervical vertebrae showed different evolutionary patterns, the atlas of hominines displayed a certain degree of homoplasy, and the subaxial cervical vertebrae a more directional-like mode of evolution. This indicates a relative morphological and evolutionary stasis in the atlas and axis regarding the rest of the cervical vertebrae, especially those located in the middle of the cervical spine (i.e., C4–C5). Fifth, as expected, removing the effect of size resulted in a reduction of the degree of craniocervical integration in all vertebrae except in the atlas. Indeed, all the cervical vertebrae except the atlas yielded significant shape variation explained by cranial size.

In sum, although the pattern of integration is relatively constant in mammals, we observed in our results subtle differences in the craniocervical pattern and magnitude of integration between humans and gorillas and chimpanzees. These differences are mainly circumscribed to cranial and cervical characters implicated in maintaining head balance. However, whether these relative differences are related to postural and/or locomotor factors is something that requires more specific analyses to be answered. Finally, we also found that the module comprising the atlas and axis reflects a certain degree of lower magnitude of shape change during evolution with the rest of the craniocervical complex.

Declaration of competing interest

None.

Acknowledgments

We would like to express our gratitude for access and technical help with the collections to Patrice Courtaud (Université de Bordeaux), Jacques Cuisin (MNHN, Paris), Emmanuel Gilissen and Wim Wendelen (Royal Museum for Central Africa, Tervuren), Olivier S. G. Pauwels and Patrick Semal (Royal Belgian Institute of Natural Sciences), Javier Quesada (Nat-Museu de Ciències Naturals, Barcelona), and Inbal Livne (Powell-Cotton Museum, Birchington, UK). This research has also received support from the Spanish Ministry of Science and Innovation through the "María de Maeztu" excellence accreditation (CEX2019-000945- M), FEDER/Ministerio de Ciencia e Innovación-Agencia Estatal de Investigación (project PGC2018-093925-B-C33), Research Group IT1418-19 from the Eusko Jaurlaritza-Gobierno Vasco, AGAUR (Ref. 2017SGR1040) and URV (Ref. 2019PFR-URV-91). A.G.O. was supported by the Ramón y Cajal fellowship (RYC-2017-22558).

Supplementary Online Material

Supplementary Online Material to this article can be found online at https://doi.org/10.1016/j.jhevol.2021.103112.

References

Ackland, D.C., Merritt, J.S., Pandy, M.G., 2011. Moment arms of the human neck muscles in flexion, bending and rotation. J. Biomech. 44, 475–486.
Adams, D.C., 2014. A generalized *K* statistic for estimating phylogenetic signal from shape and other high-dimensional multivariate data. Syst. Biol. 63, 685–697.
Adams, D.C., Nistri, A., 2010. Ontogenetic convergence and evolution of foot morphology in European cave salamanders (Family: Plethodontidae). BMC Evol. Biol. 10, 1–10.
Adams, D.C., Felice, R.N., 2014. Assessing trait covariation and morphological integration on phylogenies using evolutionary covariance matrices. PLoS One 9, e94335.
Adams, D.C., Collyer, M.L., 2016. On the comparison of the strength of morphological integration across morphometric datasets. Evolution 70, 2623–2631.
Adams, D.C., Collyer, M.L., 2019. Comparing the strength of modular signal, and evaluating alter native modular hypotheses, using covariance ratio effect sizes with morphometric data. Evolution 73, 2352–2367.
Adams, D.C., Collyer, M., Kaliontzopoulou, A., 2020. Geomorph: Software for geometric morphometric analyses. R package version 3.2.1. https://cran.r-project.org/package=geomorph.
Adams, L.M., Moore, W.J., 1975. Biomechanical appraisal of some skeletal features associated with head balance and posture in the Hominoidea. Acta Anat. 92, 580–584.
Arlegi, M., Gómez-Olivencia, A., Albessard, L., Martínez, I., Balzeau, A., Arsuaga, J.L., Been, E., 2017. The role of allometry and posture in the evolution of the hominin subaxial cervical spine. J. Hum. Evol. 104, 80–99.
Arlegi, M., Gómez-Robles, A., Gómez-Olivencia, A., 2018. Morphological integration in the gorilla, chimpanzee, and human neck. Am. J. Phys. Anthropol. 166, 408–416.
Arlegi, M., Veschambre-Couture, C., Gómez-Olivencia, A., 2020. Evolutionary selection and morphological integration in the vertebral column of modern humans. Am. J. Phys. Anthropol. 171, 17–36.
Arnold, C., Matthews, L.J., Nunn, C.L., 2010. The 10kTrees website: A new online resource for primate phylogeny. Evol. Anthropol. 19, 114–118.
Arnold, P., 2020. Evolution of the mammalian neck from developmental, morphofunctional, and paleontological perspectives. J. Mamm. Evol. 1–11.
Arnold, P., Forterre, F., Lang, J., Fischer, M.S., 2016. Morphological disparity, conservatism, and integration in the canine lower cervical spine: Insights into mammalian neck function and regionalization. Mamm. Biol. 81, 153–162.
Arnold, P., Amson, E., Fischer, M.S., 2017b. Differential scaling patterns of vertebrae and the evolution of neck length in mammals. Evolution 71, 1587–1599.
Arnold, P., Esteve-Altava, B., Fischer, M.S., 2017a. Musculoskeletal networks reveal topological disparity in mammalian neck evolution. BMC Evol. Biol. 17, 1–18.
Bardua, C., Wilkinson, M., Gower, D.J., Sherratt, E., Goswami, A., 2019. Morphological evolution and modularity of the caecilian skull. BMC Evol. Biol. 19, 1–23.
Bastir, M., Higuero, A., Ríos, L., García-Martínez, D., 2014. Three-dimensional analysis of sexual dimorphism in human thoracic vertebrae: Implications for the respiratory system and spine morphology. Am. J. Phys. Anthropol. 155, 513–521.
Bastir, M., García Martínez, D., Rios, L., Higuero, A., Barash, A., Martelli, S., García-Tabernero, A., Estalrrich, A., Huguet, R., de la Rasilla, M., Rosas, A., 2017. Three-dimensional morphometrics of thoracic vertebrae in Neanderthals and the fossil evidence from El Sidrón (Asturias, Northern Spain). J. Hum. Evol. 108, 47–61.
Bateson, W., 1894. Materials for the Study of Variation Treated with Especial Regard to Discontinuity in the Origin of Species. Macmillan, London.
Been, E., Gómez-Olivencia, A., Kramer, P.A., 2012. Lumbar lordosis of extinct hominins. Am. J. Phys. Anthropol. 147, 64–77.
Been, E., Gómez-Olivencia, A., Kramer, P.A., 2014. Brief Communication: Lumbar lordosis in extinct hominins: Implications of the pelvic incidence. Am. J. Phys. Anthropol. 154, 307–314.
Been, E., Gómez-Olivencia, A., Shefi, S., Soudack, M., Bastir, M., Barash, A., 2017. Evolution of spinopelvic alignment in hominins. Anat. Rec. 300, 900–911.

de Beer, G.R., 1937. The Development of the Vertebrate Skull. Oxford University Press, London.
Benoit, J., Legendre, L.J., Farke, A.A., Neenan, J.M., Mennecart, B., Costeur, L., Merigeaud, P., Manger, P.R., 2020. A test of the lateral semicircular canal correlation to head posture, diet and other biological traits in "ungulate" mammals. Sci. Rep. 10, 1–22.
Böhmer, C., 2017. Correlation between *Hox* code and vertebral morphology in the mouse: Towards a universal model for Synapsida. Zool. Lett. 3, 1–11.
Böhmer, C., Amson, E., Arnold, P., van Heteren, A.H., Nyakatura, J.A., 2018. Homeotic transformations reflect departure from the mammalian 'rule of seven' cervical vertebrae in sloths: Inferences on the Hox code and morphological modularity of the mammalian neck. BMC Evol. Biol. 18, 1–11.
Bookstein, F., Sampson, P.D., Streissguth, A.P., Barr, H.M., 1990. Measuring "dose" and "response" with multivariate data using partial least squares techniques. Commun. Stat. Theory Methods 19, 765–804.
Bookstein, F.L., Gunz, P., Mitteroecker, P., Prossinger, H., Schaefer, K., Seidler, H., 2003. Cranial integration in *Homo*: Singular warps analysis of the midsagittal plane in ontogeny and evolution. J. Hum. Evol. 44, 167–187.
Boyle, E.K., Mahon, V., Diogo, R., 2020. Muscles lost in our adult primate ancestors still imprint in us: On muscle evolution, development, variations, and pathologies. Mol. Biol. Rep. 6, 32–50.
Bramble, D.M., 1989. Axial-appendicular dynamics and the integration of breathing and gait in mammal. Am. Zool. 29, 171–186.
Bramble, D.M., Lieberman, D.E., 2004. Endurance running and the evolution of *Homo*. Nature 432, 345–352.
Bräuer, G., 1988. Osteometrie. In: Knussmann, R. (Ed.), Anthropologie. Handbuch der vergleichenden Biologie des Menschen. Gustav Fischer, Stuttgart, pp. 160–232.
Buchholtz, E.A., 2014. Crossing the frontier: A hypothesis for the origins of meristic constraint in mammalian axial patterning. Zoology 117, 64–69.
Buchholtz, E.A., Bailin, H.G., Laves, S.A., Yang, J.T., Chan, M.Y., Drozd, L.E., 2012. Fixed cervical count and the origin of the mammalian diaphragm. Evol. Dev. 14, 399–411.
Burke, A.C., Nelson, C.E., Morgan, B.A., Tabin, C., 1995. *Hox* genes and the evolution of vertebrate axial morphology. Development 121, 333–346.
Cheverud, J.M., 1996. Developmental integration and the evolution of pleiotropy. Am. Zool. 36, 44–50.
Choi, H., Keshner, E., Peterson, B.W., 2003. Musculoskeletal kinematics during voluntary head tracking movements in primate. KSME Int. J. 17, 32–39.
Coleman, M.N., 2008. What does geometric mean, mean geometrically? Assessing the utility of geometric mean and other size variables in studies of skull allometry. Am. J. Phys. Anthropol. 135, 404–415.
Collyer, M.L., Sekora, D.J., Adams, D.C., 2015. A method for analysis of phenotypic change for phenotypes described by high-dimensional data. Heredity 115, 357–365.
Collyer, M.L., Adams, D.C., 2018. RRPP: An R package for fitting linear models to high- dimensional data using residual randomization. https://besjournals.onlinelibrary.wiley.com/doi/10.1111/2041-210X.13029.
Collyer, M.L., Adams, D.C., 2021. RRPP: Linear Model Evaluation with Randomized Residuals in a Permutation Procedure. R package version 0.6.2. https://cran.r-project.org/package=RRPP.
Cromwell, R.L., Aadland-Monahan, T.K., Nelson, A.T., Stern-Sylvestre, S.M., Seder, B., 2001. Sagittal plane analysis of head, neck, and trunk kinematics and electromyographic activity during locomotion. J. Orthop. Sports Phys. 31, 255–262.
Darroch, J.N., Mosimann, J.E., 1985. Canonical and principal components of shape. Biometrika 72, 241–252.
Dean, M.C., 1985a. Comparative myology of the hominoid cranial base. Folia Primatol. 43, 234–248.
Dean, M.C., 1985b. Comparative myology of the hominoid cranial base, II. Folia Primatol. 44, 40–51.
Demes, B., 1985. Biomechanics of the primate skull base. Adv. Anat. Embryol. Cel. 94, 1–57.
Diogo, R., Abdala, V., Lonergan, N., Wood, B.A., 2008. From fish to modern humans–comparative anatomy, homologies and evolution of the head and neck musculature. J. Anat. 213, 391–424.
Diogo, R., Wood, B., 2011. Soft-tissue anatomy of the primates: Phylogenetic analyses based on the muscles of the head, neck, pectoral region and upper limb, with notes on the evolution of these muscles. J. Anat. 219, 273–359.
Diogo, R., Molnar, J.L., Wood, B., 2017. Bonobo anatomy reveals stasis and mosaicism in chimpanzee evolution, and supports bonobos as the most appropriate extant mode l for the common ancestor of chimpanzees and humans. Sci. Rep. 7, 1–8.
Dunbar, D.C., Badam, G.L., 1998. Development of posture and locomotion in free-ranging primates. Neurosci. Biobehav. Rev. 22, 541–546.
Dunbar, D.C., Badam, G.L., 2000. Locomotion and posture during terminal branch feeding. Int. J. Primatol. 21, 649–669.
Dunbar, D.C., Macpherson, J.M., Simmons, R.W., Zarcades, A., 2008. Stabilization and mobility of the head, neck and trunk in horses during overground locomotion: Comparisons with humans and other primates. J. Exp. Biol. 211, 3889–3907.
Ebraheim, N.A., Patil, V., Liu, J., Haman, S.P., Yeasting, R.A., 2008. Morphometric analyses of the cervical superior facets and implications for facet dislocation. Int. Orthopaed. 32, 97e101.
Ercoli, M.D., Prevosti, F.J., Alvarez, A., 2012. Form and function within a phylogenetic framework: Locomotory habits of extant predators and some Miocene Sparassodonta (Metatheria). Zool. J. Linn. Soc. 165, 224–251.
Esteve-Altava, B., Diogo, R., Smith, C., Boughner, J.C., Rasskin-Gutman, D., 2015. Anatomical networks reveal the musculoskeletal modularity of the human head. Sci. Rep. 5, 1–6.
Evans, F.G., 1939. The morphology and functional evolution of the atlas-axis complex from fish to mammals. N. Y. Acad. Sci. 39, 29–104.
Felsenstein, J., 1985. Phylogenies and the comparative method. Am. Nat. 125, 1–15.
Francis, C.C., 1955a. Dimensions of the cervical vertebrae. Anat. Rec. 122, 603–609.
Francis, C.C., 1955b. Variations in the articular facets of the cervical vertebrae. Anat. Rec. 122, 589–602.
Galis, F., 1999a. On the homology of structures and *Hox* genes: The vertebral column. In: Bock, G.R., Cardew, G. (Eds.), Homology. Academic Press, Chichester, pp. 80–94.
Galis, F., 1999b. Why do almost all mammals have seven cervical vertebrae? Developmental constraints, *Hox* genes, and cancer. J. Exp. Zool. 285, 19–26.
Gilbert, C.C., Frost, S.R., Strait, D.S., 2009. Allometry, sexual dimorphism, and phylogeny: A cladistic analysis of extant African papionins using craniodental data. J. Hum. Evol. 57, 298–320.
Gómez-Olivencia, A., Been, E., Arsuaga, J.L., Stock, J.T., 2013. The Neandertal vertebral column 1: The cervical spine. J. Hum. Evol. 64, 608–630.
Gómez-Olivencia, A., Arlegi, M., Barash, A., Stock, J.T., Been, E., 2017. The Neandertal vertebral column 2: The lumbar spine. J. Hum. Evol. 106, 84–101.
Gómez-Olivencia, A., Barash, A., García-Martínez, D., Arlegi, M., Kramer, P., Bastir, M., Been, E., 2018. 3D virtual reconstruction of the Kebara 2 Neandertal thorax. Nat. Commun. 9, 4387.
Gómez-Robles, A., Polly, P.D., 2012. Morphological integration in the hominin dentition: Evolutionary, developmental, and functional factors. Evolution 66, 1024–1043.
Goswami, A., 2006. Cranial modularity shifts during mammalian evolution. Am. Nat. 168, 270–280.
Goswami, A., Polly, P.D., 2010. The influence of modularity on cranial morphological disparity in Carnivora and Primates (Mammalia). PLoS One 5, e9517.
Goswami, A., Smaers, J.B., Soligo, C., Polly, P.D., 2014. The macroevolutionary consequences of phenotypic integration: From development to deep time. Phil. Trans. R. Soc. Lond. B 369, 20130254.
Grabowski, M.W., Polk, J.D., Roseman, C.C., 2011. Divergent patterns of integration and reduced constraint in the human hip and the origins of bipedalism. Evolution 65, 1336–1356.
Grabowski, M., Roseman, C.C., 2015. Complex and changing patterns of natural selection explain the evolution of the human hip. J. Hum. Evol. 85, 94–110.
Graf, W., Wilson, V.J., 1989. Afferents and efferents of the vestibular nuclei: The necessity of context-specific interpretation. Prog. Brain Res. 80, 149–157.
Graf, W., de Waele, C., Vidal, P.P., 1995b. Functional anatomy of the head-neck movement system of quadrupedal and bipedal mammals. J. Anat. 186, 55.
Graf, W., de Waele, C., Vidal, P.P., Wang, D.H., Evinger, C., 1995a. The orientation of the cervical vertebral column in unrestrained awake animals. Brain Behav. Evol. 45, 209–231.
Hallgrímsson, B., Willmore, K., Hall, B.K., 2002. Canalization, developmental stability, and morphological integration in primate limbs. Am. J. Phys. Anthropol. 131–158.
Hallgrímsson, B., Lieberman, D.E., Liu, W., Ford-Hutchinson, A.F., Jirik, F.R., 2007. Epigenetic interactions and the structure of phenotypic variation in the cranium. Evol. Dev. 9, 76–91.
Howells, W.W., 1973. Cranial Variation in Man. A Study by Multivariate Analysis of Patterns of Differences Among Recent Human Populations. Papers of the Peabody Museum of Archeology and Ethnology 67, 259. Peabody Museum, Cambridge.
Hutchinson, J.R., 2012. On the inference of function from structure using biomechanical modelling and simulation of extinct organisms. Biol. Lett. 8, 115–118.
Jenkins Jr., F.A., 1969. The evolution and development of the dens of the mammalian axis. Anat. Rec. 164, 173–184.
Johnson, D.R., O'Higgins, P., 1996. Is there a link between changes in the vertebral "hoxcode" and the shape of vertebrae? A quantitative study of shape change in the cervical vertebral column of mice. J. Theor. Biol. 183, 89–93.
Jorissen, C., Paillet, E., Scholliers, J., Aerts, P., Goyens, J., 2020. Head stabilization in small vertebrates that run at high frequencies with a sprawled posture. Biol. J. Linn. Soc. 130, 195–204.
Jungers, W.L., Falsetti, A.B., Wall, C.E., 1995. Shape, relative size, and size-adjustments in morphometrics. Am. J. Phys. Anthropol. 38, 137–161.
Kapandji, I.A., 1974. The physiology of the joints. In: The Trunk and Vertebral Column, vol. 3. Churchill Livingstone, Edinburgh.
Kessel, M., Gruss, P., 1991. Homeotic transformations of murine vertebrae and concomitant alteration of *Hox* codes induced by retinoic acid. Cell 67, 89–104.
Klingenberg, C.P., Zaklan, S.D., 2000. Morphological integration between developmental compartments in the Drosophila wing. Evolution 54, 1273–1285.
Klingenberg, C.P., Gidaszewski, N.A., 2010. Testing and quantifying phylogenetic signals and homoplasy in morphometric data. Syst. Biol. 59, 245–261.
Lieberman, D.E., Ross, C.F., Ravosa, M.J., 2000. The primate cranial base: Ontogeny, function, and integration. Am. J. Phys. Anthropol. 113, 117–169.
Lieberman, D.E., 2011. The Evolution of the Human Head. Harvard University Press, Cambridge.
Lockwood, C.A., Kimbel, W.H., Lynch, J.M., 2004. Morphometrics and hominoid phylogeny: Support for a chimpanzee human clade and differentiation among great ape subspecies. Proc. Natl. Acad. Sci. USA 101, 4356–4360.
Lovejoy, C.O., Latimer, B., Suwa, G., Asfaw, B., White, T.D., 2009a. Combining prehension and propulsion: The foot of *Ardipithecus ramidus*. Science 326, 72–72e8.

Lovejoy, C.O., Sewa, G., Spurlock, L., Asfaw, B., White, T.D., 2009b. The pelvis and femur of *Ardipithecus ramidus*: The emergence of upright walking. Science 326, 71e1–71e6.
Lovejoy, C.O., Simpson, S.W., White, T.D., Asfaw, B., Suwa, G., 2009c. Careful climbing in the Miocene: The forelimbs of *Ardipithecus ramidus* and humans are primitive. Science 326, 70–70e8.
Lycett, S.J., Collard, M., 2005. Do homologies impede phylogenetic analyses of the fossil hominids? An assessment based on extant papionin craniodental morphology. J. Hum. Evol. 49, 618–642.
Manfreda, E., Mitteroecker, P., Bookstein, F.L., Schaefer, K., 2006. Functional morphology of the first cervical vertebra in humans and nonhuman primates. Anat. Rec. 289B, 184–194.
Marroig, G., Cheverud, J.M., 2001. A comparison of phenotypic variation and covariation patterns and the role of phylogeny, ecology, and ontogeny during cranial evolution of New World monkeys. Evolution 55, 2576–2600.
Marroig, G., Shirai, L.T., Porto, A., de Oliveira, F.B., De Conto, V., 2009. The evolution of modularity in the mammalian skull II: Evolutionary consequences. Evol. Biol. 36, 136–148.
Martin, R., Saller, K., 1957. Lehrbuch der Anthropologie. Gustav Fischer, Stuttgart.
McCown, T.D., Keith, A., 1939. The Stone Age of Mount Carmel. The Fossil Human Remains from the Levalloiso-Mousterian. Clarendon Press, Oxford.
Melo, D., Garcia, G., Hubbe, A., Assis, A.P., Marroig, G., 2016. EvolQR: An R package for evolutionary quantitative genetics. F1000Research 4, 1–25.
Meyer, M.R., Woodward, C., Tims, A., Bastir, M., 2018. Neck function in early hominins and suspensory primates: Insights from the uncinate process. Am. J. Phys. Anthropol. 166, 613–637.
Mitteroecker, P., Bookstein, F., 2007. The conceptual and statistical relationship between modularity and morphological integration. Syst. Biol. 56, 818–836.
Müller, M.A., Merten, L.J., Böhmer, C., Nyakatura, J.A., 2021. Pushing the boundary? Testing the 'functional elongation hypothesis' of the giraffe's neck. Evolution 75, 641–655.
Nalley, T.K., Grider-Potter, N., 2015. Functional morphology of the primate head and neck. Am. J. Phys. Anthropol. 156, 531–542.
Nalley, T.K., Grider-Potter, N., 2017. Functional analyses of the primate upper cervical vertebral column. J. Hum. Evol. 107, 19–35.
Nalley, T.K., Grider-Potter, N., 2019. Vertebral morphology in relation to head posture and locomotion I: The cervical spine. In: Been, E., Gómez-Olivencia, A., Kramer, P.A. (Eds.), Spinal Evolution: Morphology, Function, and Pathology of the Spine in Hominoid Evolution. Springer International Publishing, Cham, pp. 35–50.
Narita, Y., Kuratani, S., 2005. Evolution of the vertebral formulae in mammals: A perspective on developmental constraints. J. Exp. Zool. Part B Mol. Dev. Evol. 304B, 91–106.
Olson, E.C., Miller, R.L., 1958. Morphological Integration. The University of Chicago Press, Chicago.
Pablos, A., Martínez, I., Lorenzo, C., Gracia, A., Sala, N., Arsuaga, J.L., 2013. Human talus bones from the Middle Pleistocene site of Sima de los Huesos (Sierra de Atapuerca, Burgos, Spain). J. Hum. Evol. 65, 79–92.
Pontzer, H., Holloway, J.H., Raichlen, D.A., Lieberman, D.E., 2009. Control and function of arm swing in human walking and running. J. Exp. Biol. 212, 523–534.
Porto, A., de Oliveira, F.B., Shirai, L.T., De Conto, V., Marroig, G., 2009. The evolution of modularity in the mammalian skull I: Morphological integration patterns and magnitudes. Evol. Biol. 36, 118–135.
Porto, A., Shirai, L.T., de Oliveira, F.B., Marroig, G., 2013. Size variation, growth strategies, and the evolution of modularity in the mammalian skull. Evolution 67, 3305–3332.
Powell, V., Esteve-Altava, B., Molnar, J., Villmoare, B., Pettit, A., Diogo, R., 2018. Primate modularity and evolution: First anatomical network analysis of primate head and neck musculoskeletal system. Sci. Rep. 8, 1–10.
Preuschoft, H., 2004. Mechanisms for the acquisition of habitual bipedality: Are there biomechanical reasons for the acquisition of upright bipedal posture? J. Anat. 204, 363–384.
Preuschoft, H., Klein, N., 2013. Torsion and bending in the neck and tail of sauropod dinosaurs and the function of cervical ribs: Insights from functional morphology and biomechanics. PLoS One 8, e78574.
Profico, A., Piras, P., Buzi, C., Di Vincenzo, F., Lattarini, F., Melchionna, M., Veneziano, A., Pasquale, R., Manzi, G., 2017. The evolution of cranial base and face in Cercopithecoidea and Hominoidea: Modularity and morphological integration. Am. J. Primatol. 79, e22721.
R Core Team, 2020. R: A language and environment for statistical computing. R Foundation for Statistical Computing, Vienna, Austria. URL. https://www.R-project.org/.
Randau, M., Cuff, A.R., Hutchinson, J.R., Pierce, S.E., Goswami, A., 2017. Regional differentiation of felid vertebral column evolution: A study of 3D shape trajectories. Org. Divers. Evol. 17, 305–319.
Robinson, J.T., 1972. Early Hominid Posture and Locomotion. The University of Chicago Press, Chicago.
Rohlf, F.J., Slice, D., 1990. Extensions of the Procrustes method for the optimal superimposition of landmarks. Syst. Biol. 39, 40–59.
Rohlf, F.J., Corti, M., 2000. Use of two-block partial least-squares to study covariation in shape. Syst. Biol. 49, 740–753.
Ryan, T.M., Sukhdeo, S., 2016. KSD-VP-1/1: Analysis of the postcranial skeleton using high-resolution computed tomography. In: Haile-Selassie, Y., Su, D.F. (Eds.), The Postcranial Anatomy of *Australopithecus afarensis*. Springer, Dordrecht, pp. 39–62.
Ryan, T.M., Carlson, K.J., Gordon, A.D., Jablonski, N., Shaw, C.N., Stock, J.T., 2018. Human-like hip joint loading in *Australopithecus africanus* and *Paranthropus robustus*. J. Hum. Evol. 121, 12–24.
Schluter, D., 1996. Adaptive radiation along genetic lines of least resistance. Evolution 50, 1766–1774.
Schultz, A.H., 1942. Conditions for balancing the head in primates. Am. J. Phys. Anthropol. 29, 483–497.
Schultz, A.H., 1961. Primatologia. Handbuch der primatenkunde. S. Karger, Basel.
Sidlauskas, B., 2008. Continuous and arrested morphological diversification in sister clades of characiform fishes: A phylomorphospace approach. Evolution 62, 3135–3156.
Slijper, E., 1946. Comparative biologic anatomical investigations on the vertebral column and spinal musculature of mammals. Tweede Sect. 17, 1–128.
Sockol, M.D., Raichlen, D.A., Pontzer, H., 2007. Chimpanzee locomotor energetics and the origin of human bipedalism. Proc. Natl. Acad. Sci. USA 104, 12265–12269.
Steppan, S.J., Phillips, P.C., Houle, D., 2002. Comparative quantitative genetics: Evolution of the G matrix. Trends Ecol. Evol. 17, 320–327.
Stern Jr., J.T., 2000. Climbing to the top: A personal memoir of *Australopithecus afarensis*. Evol. Anthropol. 9, 113–133.
Strait, D.S., 2001. Integration, phylogeny, and the hominid cranial base. Am. J. Phys. Anthropol. 114, 273–297.
Strait, D.S., Ross, C.F., 1999. Kinematic data on primate head and neck posture: Implications for the evolution of basicranial flexion and an evaluation of registration planes used in paleoanthropology. Am. J. Phys. Anthropol. 108, 205–222.
Toerien, M.J., 1957. Note on the cervical vertebrae of the La Chapelle man. S. Afr. J. Sci. 53, 447–449.
Toerien, M.J., 1961. The length and inclination of the primate cervical spinous processes. Trans. R. Soc. South Africa 36, 95–105.
Vander Linden, A., Campbell, K.M., Bryar, E.K., Santana, S.E., 2019a. Head-turning morphologies: Evolution of shape diversity in the mammalian atlas–axis complex. Evolution 73, 2060–2071.
Vander Linden, A., Hedrick, B.P., Kamilar, J.M., Dumont, E.R., 2019b. Atlas morphology, scaling and locomotor behaviour in primates, rodents and relatives (Mammalia: Euarchontoglires). Zool. J. Linnean Soc. 185, 283–299.
Varela-Lasheras, I., Bakker, A.J., van der Mije, S.D., Metz, J.A., van Alphen, J., Galis, F., 2011. Breaking evolutionary and pleiotropic constraints in mammals: On sloths, manatees and homeotic mutations. EvoDevo 2, 11.
Varón-González, C., Whelan, S., Klingenberg, C.P., 2020. Estimating phylogenies from shape and similar multidimensional data: Why it is not reliable. Syst. Biol. 69, 863–883.
Villamil, C.I., 2018. Phenotypic integration of the cervical vertebrae in the Hominoidea (Primates). Evolution 72, 490–517.
Villamil, C.I., 2021. The role of developmental rate, body size, and positional behavior in the evolution of covariation and evolvability in the cranium of strepsirrhines and catarrhines. J. Hum. Evol. 151, 102941.
Vidal, P.P., Graf, W., Berthoz, A., 1986. The orientation of the cervical vertebral column in unrestrained awake animals. Exp. Brain Res. 61, 549–559.
von Cramon-Taubadel, N., Smith, H.F., 2012. The relative congruence of cranial and genetic estimates of hominoid taxon relationships: Implications for the reconstruction of hominin phylogeny. J. Hum. Evol. 62, 640–653.
Wagner, G.P., 1988. The influence of variation and of developmental constraints on the rate of multivariate phenotypic evolution. J. Evol. Biol. 1, 45–66.
Wagner, G.P., 1996. Homologues, natural kinds and the evolution of modularity. Am. Zool. 36, 36–43.
Wagner, G.P., Schwenk, K., 2000. Evolutionarily stable configurations: Functional integration and the evolution of phenotypic stability. Evol. Biol. 31, 155–217.
Warrener, A.G., Lewton, K.L., Pontzer, H., Lieberman, D.E., 2015. A wider pelvis does not increase locomotor cost in humans, with implications for the evolution of childbirth. PLoS One 10, e0118903.
Watanabe, A., Fabre, A.C., Felice, R.N., Maisano, J.A., Müller, J., Herrel, A., Goswami, A., 2019. Ecomorphological diversification in squamates from conserved pattern of cranial integration. Proc. Natl. Acad. Sci. USA 116, 14688–14697.
Wellik, D.M., Capecchi, M.R., 2003. *Hox10* and *Hox11* genes are required to globally pattern the mammalian skeleton. Science 301, 363–367.
White, A.A., Panjabi, M.M., 1990. Clinical Biomechanics of the Spine. J. B. Lippincott, Philadelphia.
Whitcome, K.K., Shapiro, L.J., Lieberman, D.E., 2007. Fetal load and the evolution of lumbar lordosis in bipedal hominins. Nature 450, 1075–1078.
Zelditch, M.L., 1988. Ontogenetic variation in patterns of phenotypic integration in the laboratory rat. Evolution 42, 28–41.
Zubair, H.N., Chu, K.M., Johnson, J.L., Rivers, T.J., Beloozerova, I.N., 2019. Gaze coordination with strides during walking in the cat. J. Physiol. 597, 5195–5229.